Outer Membrane Vesicles Secreted by *Bacteroides fragilis* Inhibit CFTR Chloride Secretion by Human Colon Organoids

Roxanna Barnaby[1]*, Amanda Nymon[1]*, Paige Salerno[1]*, Carolyn Roche[1], Young Ah Goo[3], Byoung-Kyu Cho[3], Timothy B. Gardner[2], Zdenek Svindrych[4], Douglas J. Taatjes[5], Thomas H. Hampton[1], Benjamin Ross[1] and Bruce A. Stanton[1**]

[1]Department of Microbiology and Immunology, Geisel School of Medicine at Dartmouth, Hanover, NH, USA, [2]Center for Digestive Health, Dartmouth Hitchcock Medical Center, Lebanon, NH USA, [3]Mass Spectrometry Technology Access Center, McDonnell Genome Institute, Washington University School of Medicine, St. Louis, Missouri, USA, [4]Department of Biochemistry and Cell Biology, Geisel School of Medicine at Dartmouth, Hanover, NH, USA, and [5]Department of Pathology and Laboratory Medicine, University of Vermont, Burlington, VT USA

***Co-first authors.**

****Corresponding author:**

Bruce A. Stanton, Ph.D.
Department of Microbiology and Immunology
Geisel School of Medicine at Dartmouth
520 Remsen Building
Hanover NH 03755
Phone: 603-229-2803
Email: Bruce.A.Stanton@Dartmouth.edu

Running title: *Bacteroides fragilis* toxin

Competing interests. The author(s) declare no competing interests.

Abstract. The goals of this study were to develop a model to study host pathogen interactions in primary human colon organoids and to test the hypothesis that *Bacteroides fragilis* toxin (BFT-2) secreted in outer membrane vesicles (OMVs) modulates mucosal immunity and CFTR Cl^- secretion. Since Bacteroides species reside in mucus, OMVs are likely to represent a mechanism of communication between Bacteroides and the host. Two strains of Bacteroides were studied, Enterotoxigenic *Bacteroides fragilis* (ETBF), which produces BFT-2, and the non-toxigenic *Bacteroides fragilis* strain NCTC 9343 (NTBF) that does not produce BFT-2. We also utilized two additional strains of *Bacteroides fragilis:* one in which *bft*-2 was knocked out (ETBF Δ*bft*), and one that was engineered to contain *bft-2* (NTBF+*bft)*. We report that *Bacteroides fragilis* OMVs reduced CFTR Cl^- secretion but had no effect on tight junction or cell adhesion proteins, transepithelial resistance (TER) or cytokine secretion by primary human colon organoids. NTBF OMVs containing BFT-2 were more effective in reducing CFTR Cl^- secretion than NTBF lacking BFT-2. We conclude that OMVs secreted by Bacteroides can be an important mechanism of host pathogen interactions in the colon by reducing CFTR Cl^- secretion.

Keywords: *Bacteroides fragilis*, outer membrane vesicles, CFTR, transepithelial resistance, colon organoids

Introduction. The human gastrointestinal tract is colonized by ~100 trillion bacteria, including several members of the genus Bacteroides, which comprise approximately 30% of the microbiota [1-5]. Although *Bacteroides fragilis* (*B. fragilis*) is one of the least abundant species,

48 Enterotoxigenic *B. fragilis* (ETBF) is a pathogenic bacterium that induces diarrhea, colitis and
49 causes tumor formation through the secretion of Bacteroides fragilis toxin (BFT-2), a
50 metalloprotease [3,6-8]. Many, but not all, studies on colon cell lines have shown that recombinant
51 BFT-2 rapidly (~1-3 hrs.) causes cell damage and disrupts cell adhesion by cleaving E-
52 cadherin, a cell adhesion protein, leading to an increase in epithelial paracellular permeability,
53 IL-8 secretion [3,9-11,12], fluid secretion driven by CFTR Cl^- channels [13,14] and diarrhea [15-17].
54 However, in some studies on colon cell lines, E-cadherin remained unchanged after exposure to
55 ETBF supernatant [9]. The effect of NTBF and ETBF OMVs on IL-8 secretion and E-cadherin in
56 colon cell lines is dose, strain and time dependent [9,12,18]. It has been suggested that the BFT-2-
57 induced increase in permeability leads to paracellular movement of bacteria and bacterial
58 products from the lumen of the colon to the submucosal layer and blood, an effect that can train
59 the immune system [2]. Recombinant BFT-2 applied to the apical side of HT 29/C1, HT-29, T84,
60 CMT93 or MDCK cell lines decreases transepithelial resistance (TER) and cleaves E-cadherin
61 [9,11,15,17,19,20]. One study on the T84 colon cell line reported no effect of BFT-2 on short circuit
62 current but did report that BFT-2 reduced TER [20].

63 Many Gram-negative bacteria that reside in the mucus lining of the colon secrete outer
64 membrane vesicles (OMVs) [12,21-26] that stimulate inflammation and decrease ion transport,
65 including CFTR Cl^- secretion by epithelial cell lines [21-23,27]. Therefore, it is likely that
66 communication between *B. fragilis* and human colon cells is also mediated by the secretion of
67 OMVs and other soluble factors including MUC-2, antimicrobial peptides, and anti-inflammatory
68 cytokines [7,28,29]. However, nothing is known about the effects of BFT-2-containing OMVs
69 secreted by *Bacteroides* on primary human colon organoids.

70 In contrast to ETBF, the Nontoxigenic *B. fragilis* (NTBF) strain does not express *bft-2* and it
71 promotes gut homeostasis through the production of short-chain fatty acids and polysaccharide

72 A, stimulates barrier-protective molecules including ZO-1 and MUC-2, as well as the secretion
73 of antimicrobial peptides, and anti-inflammatory cytokines [1,7,30].

74 A recent review questioned the relevance of cell lines as models to elucidate the physiology and
75 pathophysiology of the colon since cell lines are rarely normal, and contain several mutations
76 and chromosomal defects that enable their persistence [31]. In particular, it has been reported that
77 the gene expression pattern of the Caco-2 cell line, which is studied as a surrogate of the colon,
78 was similar to that of epithelial cells of the small intestine [32]. Since, as noted above, colon cell
79 lines do not produce consistent responses to recombinant BFT-2 [3,9,10], one of the most
80 important challenges involves the assessment of BFT-2 secreted in OMVs on primary human
81 colon organoids [1]. To elucidate the biological activity of BFT-2 secreted in OMVs, we obtained
82 colon biopsies from multiple healthy human donors to develop differentiated two-dimensional
83 monolayers of primary colon organoids. Primary colon organoids contain the multiple cell
84 populations found in native tissue, compared to cell lines, which do not fully differentiate [31].
85 Accordingly, the goals of this study were to develop a model to study host pathogen interactions
86 in primary human colon organoids, and to test the hypothesis that BFT-2 secreted in OMVs
87 modulates mucosal immunity, TER and CFTR Cl^- secretion, a major driver of fluid secretion in
88 the colon [14]. We report that OMVs had no effect on cell adhesion or tight junction proteins,
89 notably E-cadherin and claudin-2, TER, or sodium reabsorption, but did inhibit forskolin-
90 stimulated CFTR Cl^- secretion, an effect predicted to decrease fluid secretion by the colon.
91 NTBF OMVs containing BFT-2 had a more inhibitory effect on CFTR Cl^- secretion by primary
92 human colonoids than NTBF OMVs lacking BFT-2. In addition, OMVs were not pro-
93 inflammatory as determined by measuring the secretion of 48 cytokines. OMVs also reduced
94 CFTR Cl^- secretion by T84 cells, a colon cell line, but did not alter TER. These results
95 demonstrate that OMVs and BFT-2 secreted by *B. fragilis* have very different biological effects
96 on primary human colon organoids compared to colon cell lines exposed to recombinant BFT-2.

97 **Results**

98 **Isolation and characterization of OMVs secreted by Bacteroides.** To test the hypothesis
99 that BFT-2 in OMVs leads to a disruption in the integrity of epithelial barriers and modulates
100 CFTR Cl^- secretion, we utilized four strains of *B. fragilis*, including ETBF and ETBF in which the
101 *bft-2* gene was deleted (ETBF Δ*bft*), NTBF, a strain that does not express *bft-2,* and NTBF in
102 which the *bft-2* gene was expressed (NTBF+*bft*). Nanoparticle tracking analysis (NTA), which
103 measures the size of vesicles by dynamic light scattering, revealed that the size of OMVs
104 isolated from bacterial cultures was similar for most strains, except that ETBF OMVs were
105 significantly smaller than NTBF OMVs (**Figure 1**).

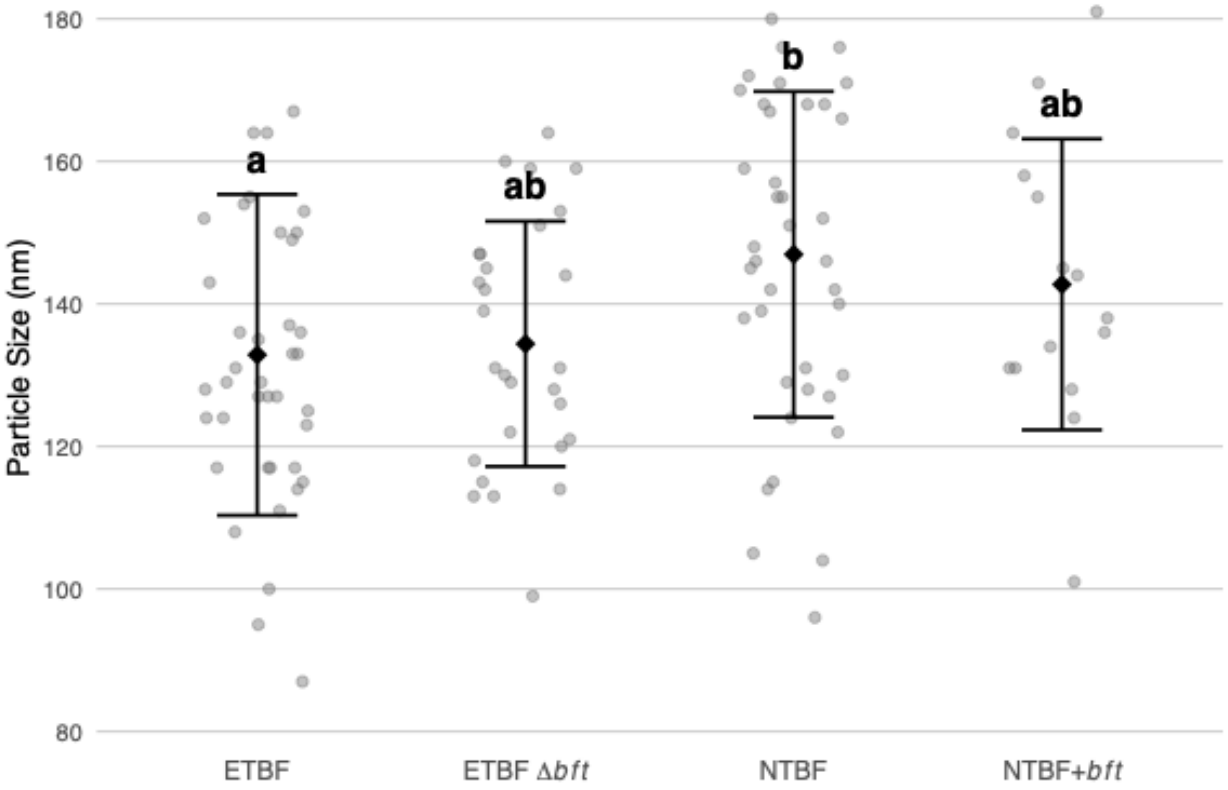

106

107 **Figure 1: Bacteroides OMV particle size determined by NTA**. Individual measurements are
108 shown as gray circles, with group means (black diamonds) and error bars (±SD). Treatments:

109 ETBF, ETBF Δ*bft*, NTBF, and NTBF+*bft*. Letters above bars indicate statistical groupings based
110 on one-way ANOVA with Tukey's HSD post-hoc test; groups sharing the same letter are not
111 significantly different (P > 0.05), while groups with different letters are significantly different (P <
112 0.05).

113

114 According to NTA analysis, the number of OMVs in each bacterial culture was: 1.4 x 10^{11}
115 particles/ml for ETBF, 2.8 x 10^{11} particles/ml for ETBF Δ*bft,* 2.0 x 10^{11} particles/ml for NTBF and
116 2.2 x 10^{11} particles/ml for NTBF+*bft*. To confirm that we isolated OMVs, transmission electron
117 microscopy (TEM) was utilized to image OMVs (**Figure 2**). OMVs were not observed in process
118 control (PC, bacterial culture media not exposed to bacteria and run through the OMV isolation
119 process); however, OMVs were observed in media isolated from ETBF, NTBF, ETBF Δ*bft* and
120 NTBF+*bft* (**Figure 2**). The mean diameter (±SEM) of OMVs as measured by TEM were similar
121 in all groups (P>0.77): ETBF [(59.0 nm ± 2.0 nm, (n=31)], ETBF Δ*bft* [(63.2 ± 3.6 nm (n=21)],
122 NTBF [(60.2 ± 4.0 nm, (n=14)] and NTBF+*bft* [(58.0 ± 5.0 nm (n=11)]. Most Bacteroides OMVs
123 had typical morphology, but we also observed some collapsed vesicular forms and the presence
124 of some irregularly shaped vesicles, similar to images published recently for Bacteroides OMVs
125 secreted by ETBF and NTBF [33]. As expected, the size of OMVs was assay dependent: dynamic
126 light scattering tends to overestimate size, whereas TEM tends to underestimate size [34,35].

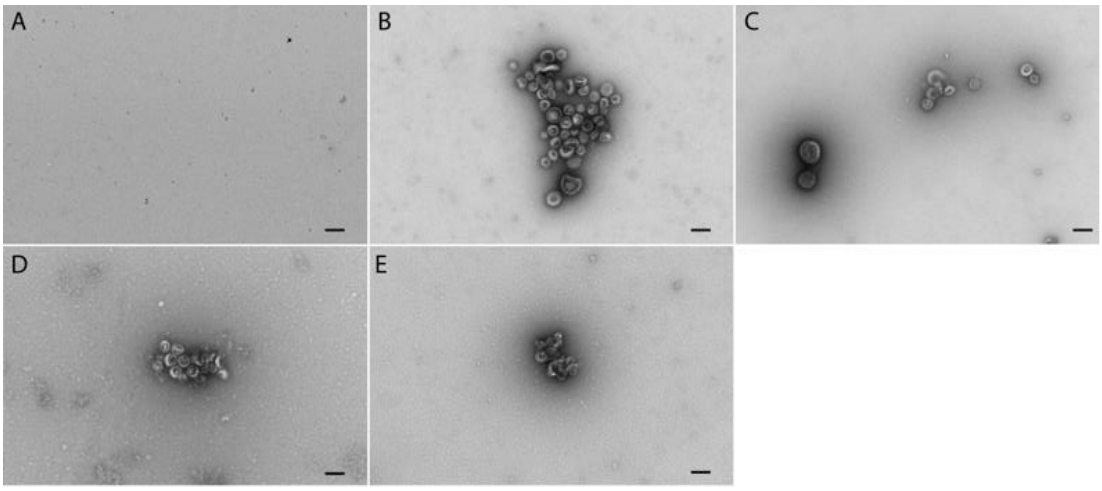

127

128 **Figure 2. Representative transmission electron microscopy images of negatively stained**
129 **Bacteroides OMVs.** (A) Process control. (B) ETBF. (C) ETBF Δ*bft*. D. NTBF. E. NTBF+*bft*.
130 Images taken by an observed blinded to the origin of the OMVs. Scale bars 100 nm.

131

132 Analysis of the proteome of OMVs was conducted to confirm that BFT-2 was present in ETBF
133 and NTBF+*bft* and absent in ETBF Δ*bft* and NTBF. Results of the proteomics analysis of OMVs
134 are presented in **Figure 3 and** Supplemental Tables 1-4. We detected 568 proteins in NTBF
135 OMVs and 437 proteins in ETBF OMVs, with 247 proteins being found in both strains. The
136 amount of BFT-2 was similar in ETBF OMVs and NTBF+*bft* OMVs as determined by intensity-
137 based quantification ($\log_2$ 12.43 for NTBF+*bft* and $\log_2$ 12.90 for ETBF). BFT-2 could not be
138 detected by proteomic analysis in NTBF and ETBF Δ*bft* OMVs.

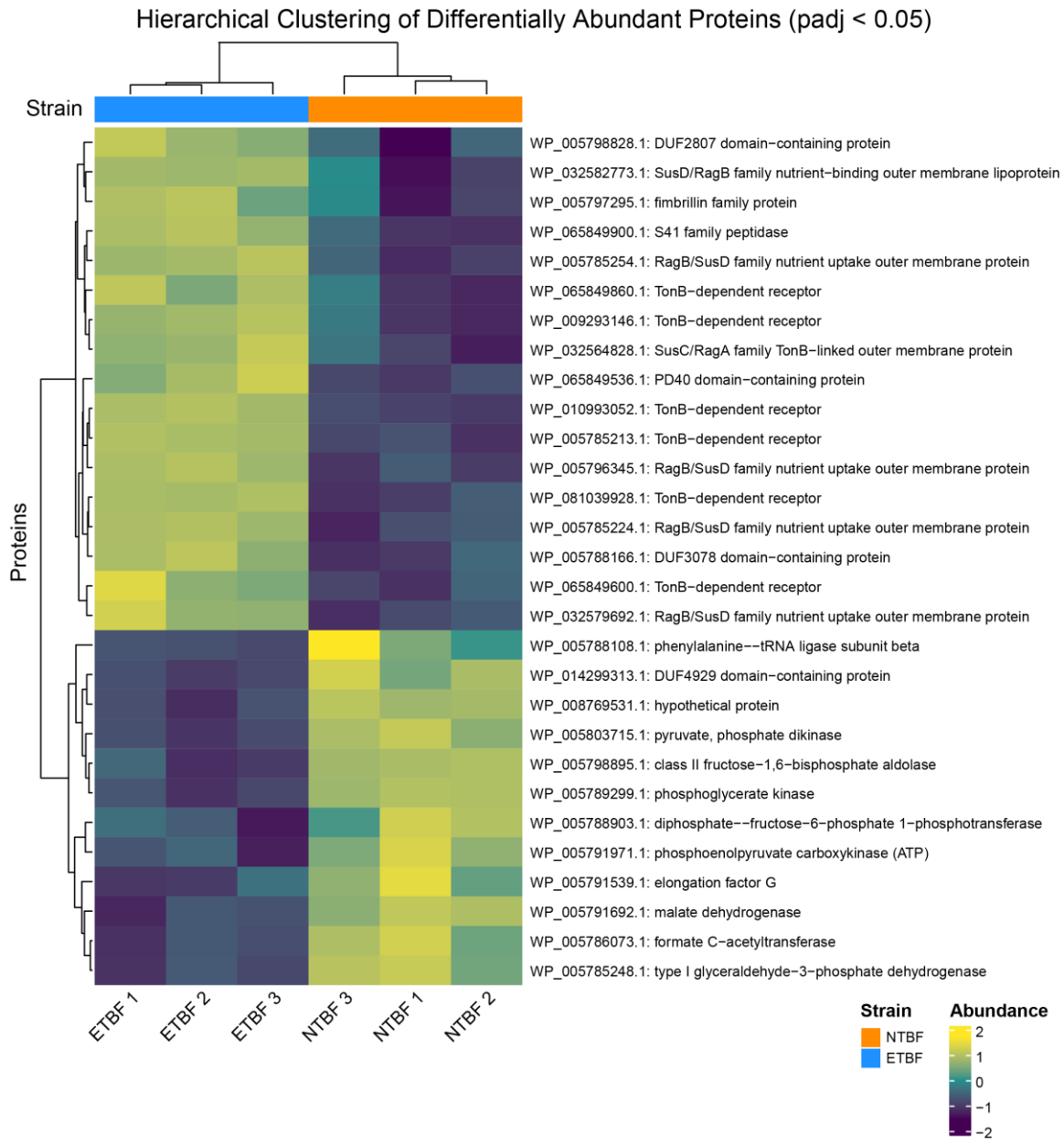

Figure 3. ETBF and NTBF OMV proteomes. Differential abundance analysis reveals significant differences between the proteome of ETBF and NTBF OMVs. The list of all identified proteins by proteomics analysis are presented in the Supplemental Tables. Supplemental Table 1 includes proteins detected exclusively in NTBF OMVs. Supplemental Table 2 includes proteins detected exclusively in ETBF OMVs. Supplemental Table 3 includes proteins detected in both ETBF and NTBF OMVs. Finally, Supplemental Table 4 includes differential expression of

146 proteins in ETBF and NTBF OMVs, the results of which are depicted in this Figure. In
147 accordance with previous research, our results show several TonB dependent receptors are
148 more abundant in OMVs secreted by ETBF compared to NTBF strains [36].

149

150 **Characterization of primary human colon organoids: Development of a model to study**
151 **host pathogen interactions in the colon.** Biopsies of human proximal colon were obtained
152 during clinical colonoscopy after obtaining informed consent from healthy volunteers at
153 Dartmouth Health. As described in methods, crypt cells were dispersed and grown in Matrigel
154 until 3D colon organoids were formed. 3D colon organoids were then seeded on Transwell
155 filters and grown for one week to develop polarized and differentiated colon organoids. We used
156 an imaging approach to characterize the cellular composition of colon organoids *in vitro* as
157 monolayers. **Figures 4-5** reveal that the colon organoids contain cell types found in the proximal
158 colon including mucin (MUC2) producing cells, CFTR expressing cells, SLC26A3 expressing
159 cells, and enterochromaffin cells [14,37]. These observations indicate that the human primary colon
160 organoids are a well differentiated epithelium, have similar cell types to the colon *in vivo* and are
161 a new model to study host pathogen interactions [14,37].

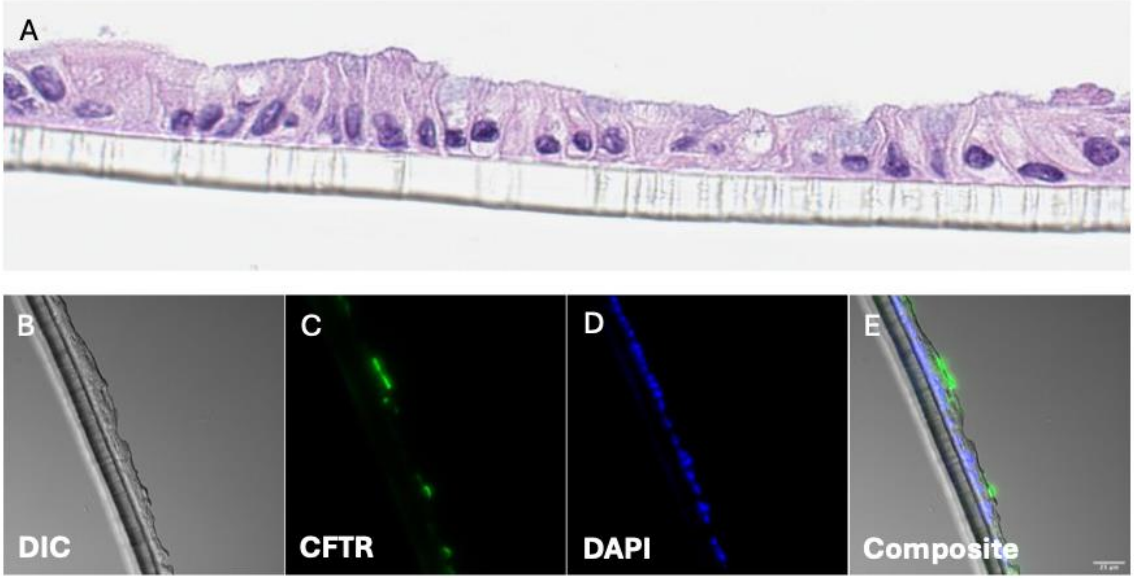

162

163 **Figure 4. Representative images of human colon organoids.** (A) Cross section of a
164 confluent monolayer of colon organoids grown on Transwell filters (10 μm thick: H&E-stained
165 cells). (B) differential contrast (DIC) image of a 6 μm thick frozen cross-section of differentiated
166 colon organoids on Transwell filters. (C) Image of the same colon organoid as in B but
167 immunofluorescent image of CFTR. (D) DAPI nuclear labeling of the same colon organoid
168 monolayer as in B and C. (E) Composite of B-D showing apical membrane labeling of CFTR.
169 Scale bar in panel E is 50 μm.

170

171 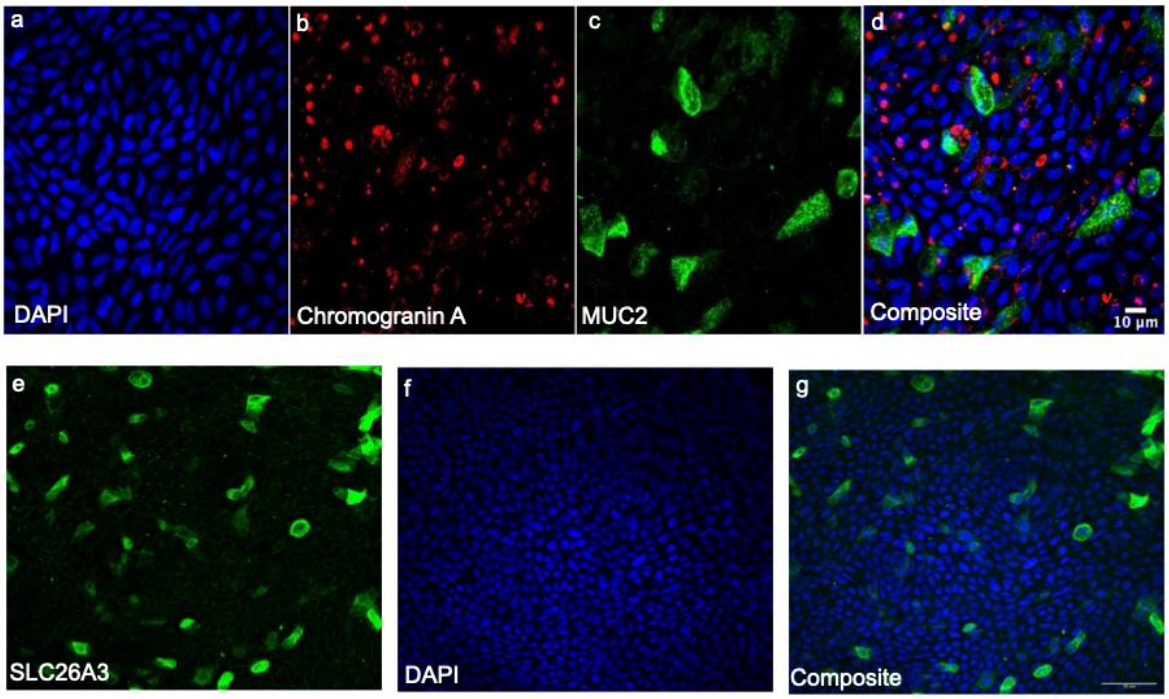

172 **Figure 5. Representative *en face* images of human colon organoids on Transwell filters.**
173 (a) DAPI labeling of nuclei. (b) Chromogranin A immunofluorescence of enterochromaffin cells.
174 (c) Immunofluorescence of MUC2. (d) Composite of A-C revealing that MUC2 and
175 Chromogranin A are expressed in different cell types. (e) Immunofluorescence of SLC26A3
176 (DRA, a Cl^-/HCO^-_3 exchanger). (f) DAPI labeling of nuclei. (g) Composite of e and f. Scale bar in
177 panel g is 50 μm.

178

179 **OMVs inhibit CFTR Cl^- secretion by primary human colon organoids**. Previous studies
180 have shown that recombinant BFT-2 stimulates CFTR Cl^- secretion, when added to the
181 basolateral side of T84 cells [20]. To examine the effect of OMVs secreted by *B. fragilis* on CFTR
182 Cl^- secretion by primary human colon organoids, OMVs were isolated and applied to the apical
183 side (the side of the colon exposed to Bacteroides *in vivo*) of colon organoids for 1 hr. and then
184 forskolin-stimulated CFTR Cl^- secretion was measured in Ussing chambers immediately after
185 the 1 hr. exposure, or 24 hrs. after washing the OMVs from the organoids. Forskolin increases

186 the activity of protein kinase A, which phosphorylates and activates CFTR Cl^- secretion [38].

187 **Figure 6** demonstrates that OMVs secreted by ETBF, ETBF Δ*bft* and NTBF+*bft* reduced

188 forskolin stimulated CFTR Cl^- secretion after 1 hr. of exposure compared to process control

189 (PC). Notably, OMVs secreted by ETBF reduced Cl^- secretion significantly more than OMVs

190 secreted by NTBF that does not express BFT-2. Expression of *bft* in NTBF (NTBF+*bft*) reduced

191 CFTR Cl^- secretion compared to NTBF OMVs, which do not express BFT-2.

192 Twenty-four hrs. after a 1 hr. exposure to OMVs, CFTR Cl^- secretion was not significantly

193 reduced by ETBF, ETBF Δ*bft*, or NTBF when compared to PC (**Figure 6**). However, 24 hrs.

194 after exposure to NTBF+*bft* OMVs, CFTR Cl^- secretion was less that CFTR Cl^- secretion

195 compared to NTBF OMVs (**Figure 6**).

196 OMVs had no effect on the amiloride-sensitive short circuit Na^+ currents (Isc, μA/cm^2), either

197 after a 1 hr. exposure to OMVs or after 24 hrs. following the 1 hr. exposure to OMVs (**Figure 7**).

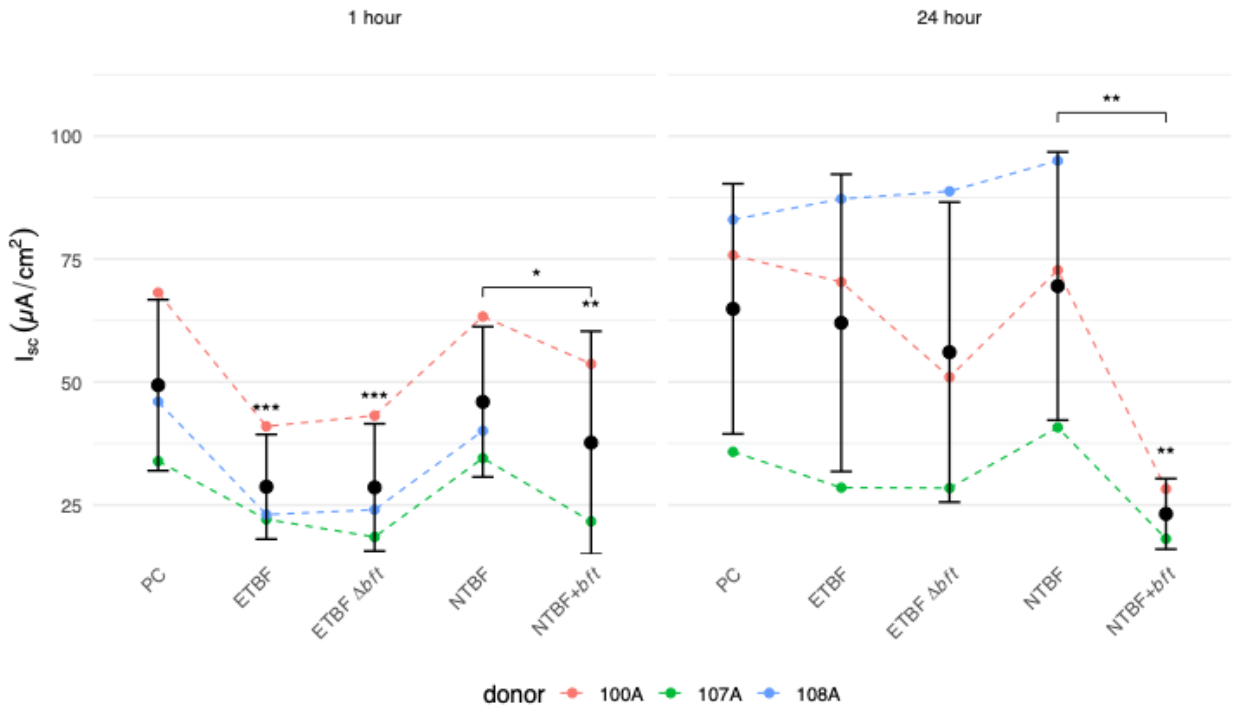

198

199 **Figure 6. CFTR Cl^- secretion by human primary colon organoids measured as short**
200 **circuit current** (Isc, μA/cm^2). Left: 1 hr. after exposure to PC or OMVs (2×10^{10}/ml OMVs, a
201 concentration of OMVs similar to that measured in conditioned media and in biological fluids
202 [21,39]). Right: 24 hrs. after a 1 hr. exposure to PC or OMVs (2×10^{10}/ml). Individual donor
203 responses are shown as dashed colored lines, with each color representing a different donor (n
204 = 3 donors; Donor 108A is female, Donors 100A and 107A are male). Solid black lines connect
205 the mean current values across treatments. Data expressed as mean ± one standard deviation.
206 Many significant differences from PC were observed at 1 hr. (ETBF, ***P = 0.00014; ETBF Δ*bft*,
207 ***P = 0.00014; and NTBF+*bft*, **P = 0.0030). Expression of *bft* in NTBF (NTBF+*bft)* OMVs
208 reduced CFTR Cl^- secretion at 1 hr. compared to NTBF OMVs, as indicated by the horizontal
209 bar (**P = 0.01200). At 24 hrs. only NTBF+*bft* OMVs reduced CFTR Cl^- secretion compared to
210 PC (P=0.008). The horizontal bar indictes that NTBF+*bft* OMVs significantly reduced CFTR Cl^-
211 secretion (**P = 0.004) compared to NTBF OMVs. Statistical analysis was performed using
212 mixed-effects linear models with donor as a random effect for each time point separately.
213 Experiments done with three donors of colon cells, three technical replicates per donor and
214 three different preparations of OMVs. Technical replicates were averaged as a single data point.

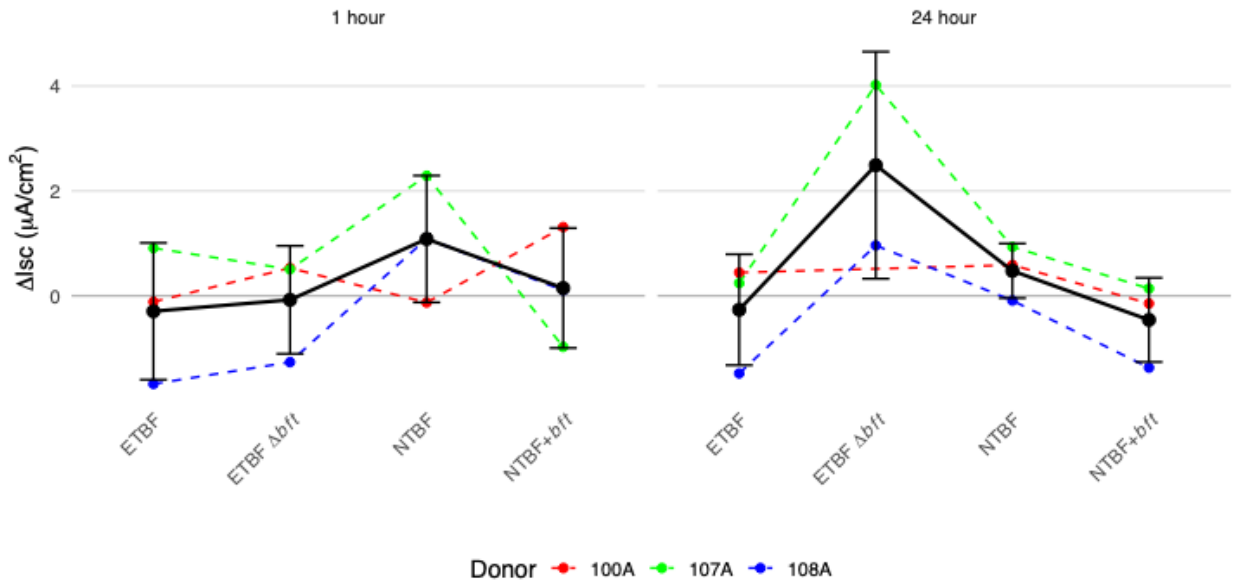

215

216 **Figure 7. OMVs did not modify amiloride-sensitive short circuit Na^+ currents**. Amiloride-
217 sensitive Na^+ currents in response to OMVs (2×10^{10}/ml OMVs) compared to PC. The difference
218 in amiloride-sensitive currents (ΔIsc) between PC and OMVs exposed colon organoids is
219 plotted. Colon organoids were exposed to OMVs for 1 hr. or 24 hrs. Each measurement of
220 amiloride-sensitive current for each donor was adjusted by subtracting the Process Control (PC)
221 current from the same Ussing chamber session and the same donor. Data from each donor
222 (100A = red, 107A = green, 108A = blue) is depicted with dashed lines. The Isc OMVs vs. PC)
223 for all donors is shown with a solid black line with ± one standard deviation. The horizontal line
224 at zero represents no change from PC. Statistical analysis was performed using mixed-effects
225 linear models with donor as a random effect for each time point separately. Experiments done
226 with three donors of colon cells, three technical replicates per donor and three different
227 preparations of OMVs. Technical replicates were averaged as a single data point.

228

229 Experiments were also conducted to determine if OMVs had an effect on TER, since previous
230 studies have shown that recombinant BFT-2 reduced TER in several colon cell lines [9,15,17,19,20].

231 However, none of the OMVs had a significant effect on TER (**Figure 8**) compared to process
232 control (PC) at 1 hr. and 24 hrs.

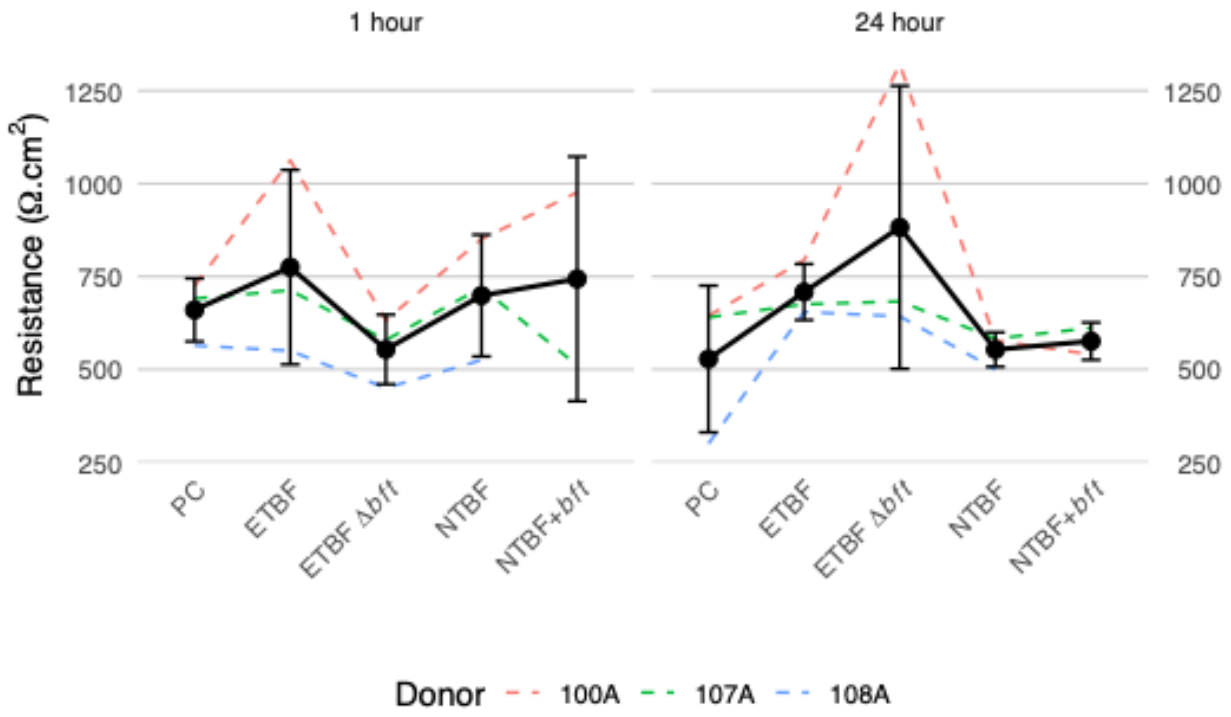

233

234 **Figure 8. Transepithelial resistance (TER) of primary human colon organoids**. TER was
235 measured in colon organoids in which CFTR Cl^- secretion was measured 1 hr. (left figure) or 24
236 hrs. (right figure) after exposure to PC or OMVs (2×10^{10}/ml OMVs) secreted by ETBF, ETBF
237 Δ*bft*, NTBF and NTBF+*bft*. Individual donor responses are shown as dashed colored lines, with
238 each color representing a different donor. Solid black lines connect the mean TER values
239 across treatments. Data expressed as mean ± one standard deviation. Statistical analysis was
240 performed using mixed-effects linear models with donor as a random effect for each time point
241 separately. Experiments done with three donors of colon cells, three technical replicates per
242 donor and three different preparations of OMVs. Technical replicates were averaged as a single
243 data point. No significant differences compared to PC (1hr. and 24 hr. exposure) were observed
244 ($P>0.05$).

245

246 **Bacteroides reduces CFTR Cl^- secretion by T84 cells but has no effect on TER.** We also
247 conducted studies on T84 cells, a colon cell line that has been used to study the effects of
248 recombinant BFT-2 [40-42]. Previous studies have shown that recombinant BFT-2 reduces the TER
249 in several colon cell lines [9,15,17,19,20]. To determine if *B. fragilis* OMVs also reduced TER and
250 influenced CFTR Cl^- secretion, we conducted Ussing experiments on monolayers of T84 cells
251 under conditions identical to the previously described exposure of primary human colon
252 organoids. Compared to PC, CFTR Cl^- secretion was reduced by all OMVs (**Figure 9a**). ETBF
253 OMVs were not more effective than NTBF OMVs in reducing CFTR Cl^- secretion. Moreover,
254 deletion of *bft-2* in ETBF did not significantly reduce the effect of ETBF OMVs on CFTR Cl^-
255 secretion. OMVs also had no effect on TER (**Figure 9b**). Thus, OMVs reduced CFTR Cl^-
256 secretion by both primary human colon organoids and T84 cells, without altering TER.

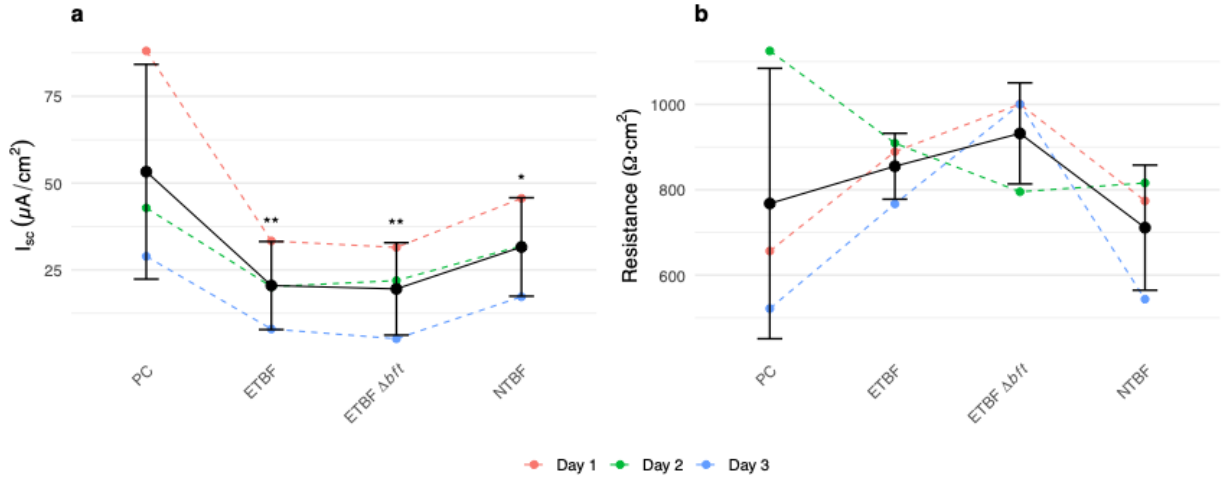

257

258 **Figure 9. CFTR Cl^- secretion and TER by T84 cells exposed to OMVs.** The protocol was
259 identical to that performed on primary human colon organoids. T84 monolayers were exposed
260 to OMVs (2×10^{10}/ml) for 1 hr. and CFTR Cl^- secretion (short-circuit current: Isc) was measured.
261 Data represent individual experiments (dashed lines) grouped by experimental date (colors) with
262 means ± one standard deviation. (a) CFTR Cl^- secretion. Each line connects experiments

263 conducted on the same day on the same pass of T84 cells. Compared to PC, CFTR Cl^-
264 secretion was significantly reduced by ETBF (**P = 0.006), ETBF Δ*bft* (**P = 0.005), and
265 NTBF (*P = 0.032) OMVs. (b) TER in the same set of T84 cells used for measurements of
266 CFTR Cl^- secretion. No significant differences in TER compared to PC were observed after 1 hr.
267 of exposure to OMVs. Statistical analysis was performed using mixed-effects linear models with
268 donor as a random effect for each time point separately. Experiments done with three different
269 preparations of OMVs. Technical replicates were averaged as a single data point.

270

271 **OMVs do not alter tight junction or cell adhesion protein abundance.** Previous studies
272 have also shown that recombinant BFT-2 rapidly (<1 hr.) reduced the expression of the cell
273 adhesion protein E-cadherin in cell lines [9,15,17,19,20]. However, we observed no effect of
274 Bacteroides OMVs on the abundance of E-cadherin or on the tight junction protein claudin-2 in
275 human colon organoids as determined by immunofluorescence microscopy (**Figure 10**).

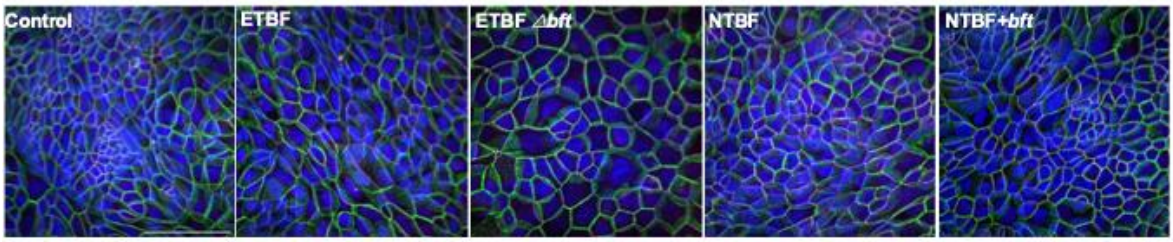

276

277 **Figure 10. Representative composite images of human colon organoids.** Organoids were
278 grown on Transwell filters and exposed to OMVs (2×10^{10}/ml) for 1 hr. Claudin-2 (magenta) and
279 E-cadherin (green) were identified by immunofluorescence. DAPI (blue) identified nuclei. Each
280 image is a composite of colon organoids labeled for claudin-2, E-cadherin and nuclei (DAPI).
281 Confocal images were analyzed by an investigator who was blinded to the treatment. There was
282 no difference in claudin-2 or E-cadherin abundance using confocal microscopy and the Fiji

283 open-source image processing package to quantify fluorescence intensity (see **Figure 11** for
284 data).

285

286 Studies were also conducted to measure E-cadherin and claudin-2 fluorescence imaged by
287 confocal microscopy. None of the OMVs had a significant effect on E-cadherin or claudin-2
288 fluorescence (**Figure 11**) confirming the immunofluorescent images in Figure 10.

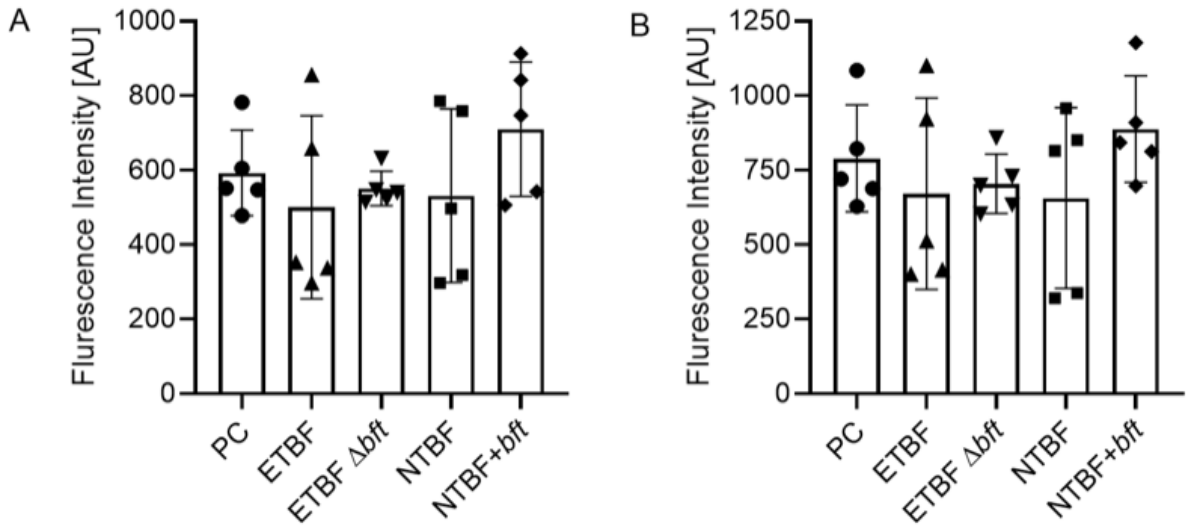

289

290 **Figure 11. Measurements of E-cadherin (A) and claudin-2 (B) epifluorescence**. Data were
291 generated by a co-author blinded to the experimental treatment. Five random images were
292 chosen for each treatment. There was no significant effect of OMVs (2×10^{10}/ml) on E-cadherin
293 or claudin-2 abundance. AU, arbitrary fluorescent units. Data expressed as mean ± one
294 standard deviation.

295

296 **Cytokine secretion by human primary colon organoids.**

297 Previous studies on cell lines and human colon tissue reported that *B. fragilis* and recombinant
298 BFT-2 stimulates IL-8 secretion [9,15,17-20]. To examine the effect of OMVs on the innate immune

299 response, colon organoids were grown on Snapwell filters and exposed to PC or OMVs in the
300 apical media for 1 hr. or 24 hrs. after OMVs were removed by washing. **Figure 12** demonstrates
301 that OMVs had no significant effect on IL-8 secretion compared to PC. Moreover, there was no
302 significant effect of any OMVs compared to PC on the secretion of 48 cytokines measured using
303 the MILLIPLEX MAP Human Cytokine/Chemokine 48-Plex cytokine assay, although there were
304 some trends in the response. For example, compared to PC, 24 hrs. after exposure to ETBF
305 OMVs, and NTBF+*bft* OMVs IL-8 increased compard to PC; however the changes were not
306 statistically significant.

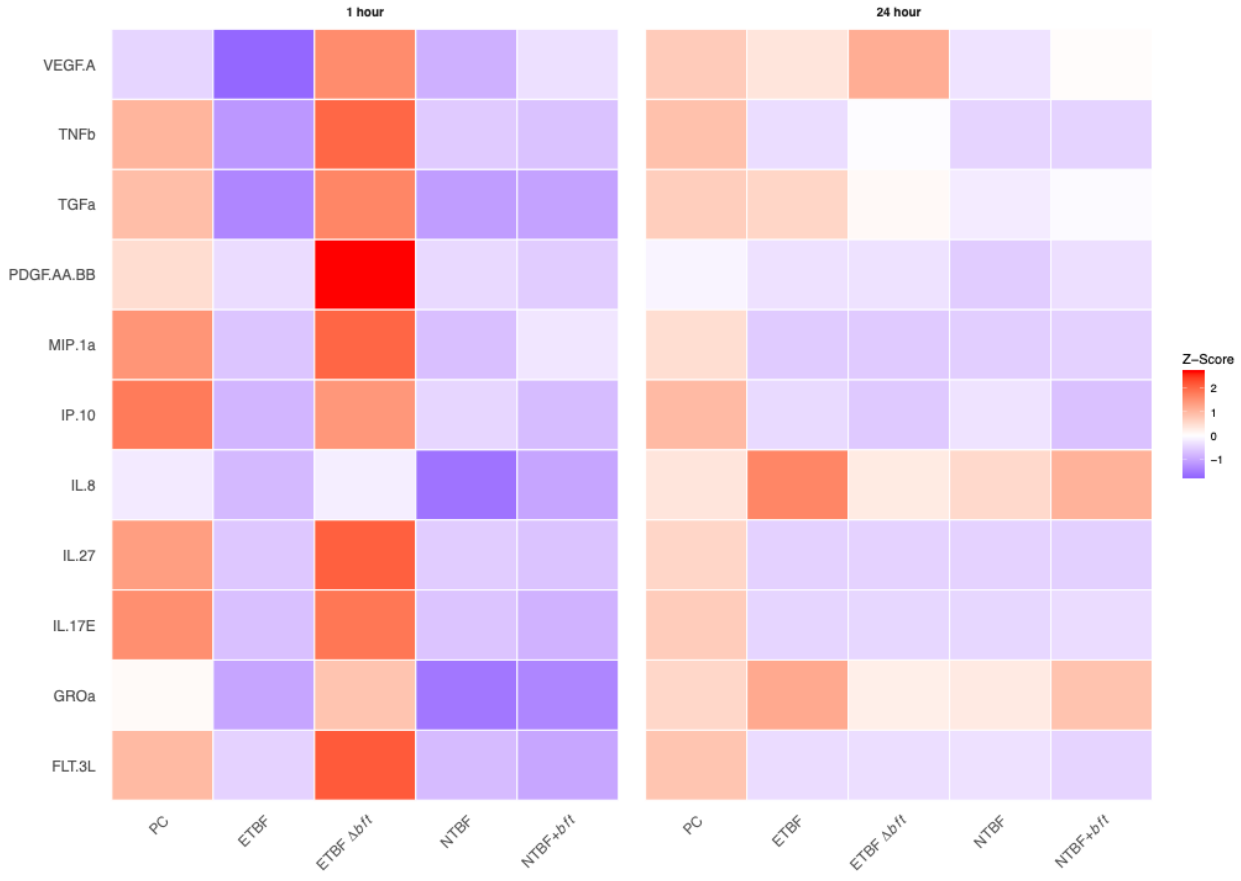

307

308 **Figure 12. Cytokine secretion following 1 hr. and 24 hrs. after exposure to OMVs secreted**
309 **by *Bacteroides fragilis* or to PC.** There were no significant effects of OMVs (2×10^{10}/ml) versus
310 PC. Values represent means across all donors (n = 3 donors) for each treatment condition.

311 Color scale indicates standard deviations from the time point mean: red represents above-
312 average expression, blue represents below-average expression, and white represents average
313 expression for each cytokine at each time point. Only cytokines with complete data (values
314 above detection) across all conditions are shown. Data were log2-transformed prior to z-score
315 calculation.

316

317 **Discussion**

318 There were two primary goals of this study: (1) To develop a well-differentiated primary culture
319 of human colon organoids and (2) to elucidate the effect of endogenous BFT-2 in OMVs
320 secreted by *B. fragilis* on human primary colon organoids. We sucessfully developed a model of
321 colon organoids from three donors that displayed a differentiated epithelium containing cell
322 types found in the proximal colon including mucin (MUC2) producing cells, CFTR expressing
323 cells, SLC26A3 (DRA, a Cl^-/HCO^-_3 exchanger that plays a key role in fluid absorption and
324 enterocyte acid/base balance) expressing cells, and enterochromaffin cells that underlie
325 epithelial cells and secrete serotonin, which stimulates GI motility and fluid and electrolyte
326 secretion [14,37]. These observations indicate that the human primary colon organoids are a
327 representative model to study host pathogen interactions in the human colon [14,37]. Studies were
328 also conducted to examine the effect of OMVs on CFTR Cl^- secretion, amiloride-sensitive
329 sodium absorption, TER, and cytokine secretion. We found that OMVs secreted by most strains
330 of Bacteroides significantly reduced CFTR Cl^- secretion by colon organoids compared to PC
331 after 1 hr. exposure. Deletion of the *bft*-2 gene from ETBF reduced the inhibitory effect of ETBF
332 OMVs on CFTR Cl^- secretion. Moreover, NTBF+*bft* OMVs were significantly more inhibitory to
333 CFTR Cl^- secretion compared to OMVs secreted by NTBF. Both observations indicate that BFT-
334 2 inhibits CFTR Cl^- section. Twenty-four hrs. after exposure to OMVs, only NTBF+*bft* OMVs
335 reduced CFTR Cl^- secretion compared to NTBF OMVs and PC. Thus, BFT-2 in OMVs was, at

336 least in part, responsible for the decrease in CFTR Cl^- secretion by primary human colon
337 organoids. Since OMVs secreted by strains of *B. fragilis* that lacked *bft*-2 (BFT Δ*bft* and NTBF)
338 also reduced CFTR Cl^- secretion, there must be other factors in OMVs including, but not limited
339 to, proteins or miRNAs that inhibit forskolin-stimulated CFTR Cl^- secretion. By contrast to results
340 from human colon organoids all OMVs secreted by *B. fragilis* inhibited CFTR Cl^- secretion by
341 T84 cells to the same extent. The reason for this difference between the effect of OMVs on T84
342 cells and human colon organoids is unknown, but it may be related to several factors, including,
343 but not limited to, possible differences in the time dependent effects of BFT-2 as well as
344 differential expression of gene and signaling pathways between T84 tumor cells and primary
345 human colon organoids. Additional studies are required to identify these factors.
346 The observation that OMVs inhibited CFTR Cl^- secretion by primary human organoids is
347 interesting to note since infection with ETBF causes secretory diarrhea, which one might expect
348 to be caused by increased CFTR Cl^- secretion, a primary driver of fluid secretion by the
349 colon[13,14]. However, there is differential expression and regulation of ion transporter proteins
350 along the length of the colon, as well as differential responses to drugs, hormones, and immune
351 factors along the length of the colon [13,14]. Accordingly, our results are applicable to the proximal
352 human colon, and other segments of the colon may react differently to OMVs and BFT-2. It is
353 the composite effect of ETBF and BFT-2 on the gastrointestinal tract that determines the
354 response *in vivo* to ETBF.
355 Our studies also did not observe a significant effect of OMVs on cytokine secretion by human
356 colon organoids. Most notably, IL-8 secretion was not significantly increased by OMVs(**Figure**
357 **12**), in contrast to studies using recombinant BFT-2 in cells lines reporting that recombinant
358 BFT-2 increased IL-8 secretion [9,15,17-20]. The reason for this difference between the effect of
359 OMVs on colon cell lines and human colon organoids is unknown, but it may be related to
360 several factors, including, but not limited to, differences in the amount of recombinant versus
361 native BFT-2 in OMVs, as well as differences in gene signaling pathways between colon cell

362 lines and human primary colon organoids. Studies have also shown that the effect of
363 recombinant BFT-2 and OMVs on colon cell lines is dose dependent, and it is likely that the
364 concentration of BFT-2 in OMVs is less that the doses of recombinant BFT-2 utilized in studies
365 on cell lines [11,18]. We conclude that biologically relevant levels of OMVs[21,39] secreted by *B.*
366 *fragilis* containing BFT-2 inhibit CFTR Cl^- secretion, but have no effect on amiloride-sensitive
367 sodium reabsorption, claudin-2, E-cadherin or TER, on primary human colonoids.

368 Fragipain was not detected in any of the OMV samples (Supplemental Table 4). Fragipain is
369 known to cleave BFT-2 into its active form [43], however, studies suggest that this protein is not
370 required for cleavage of BFT-2 in antibiotic treated mice [44]. More specifically, fragipain is
371 unnecessary when recombinant BFT-2 is mixed with the colon mucus of pathogen free or germ-
372 free mice, suggesting the mucosal activation process may be more prevalent in gastrointestinal
373 conditions containing increased mucus, such as CF [44]. Notably, primary human colon organoids
374 also secrete mucin. PBS is also able to facilitate the cleavage of BFT-2 into its active form, and
375 further suggests that fragipain is not required for BFT-2 activation [44].

376 In accordance with previous research, our proteomics data revealed that several TonB
377 dependent receptors are more abundant in OMVs secreted by ETBF compared to NTBF strains
378 (Supplemental Table 4) [45]. TonB dependent receptors are one part of outer membrane
379 structures that are critical for the influx of nutrients via SusC and SusD outer membrane
380 proteins, which were elevated in ETBF OMVs compared to NTBF OMVs [36]. An increase in
381 abundance of these proteins suggests an enhanced need for ETBF to increase nutrient
382 acquisition, thereby improving its ability to compete for similar niches that NTBF does not
383 struggle to fill. Regardless, these results pose interesting questions for mechanistic follow up
384 experiments in the future.

385 Importantly, although several studies have shown that recombinant BFT-2 degrades E cadherin
386 and claudin-2 in cell lines[9,15,17,19,20] , none of the OMVs tested herein had any effect on the

387 abundance of the tight junction protein claudin-2, the cell adhesion protein E-cadherin, or on the
388 TER. Claudin-2 is an important component of the tight junction, and reductions in claudin-2
389 abundance decrease TER[46,47]. Several possible explanations may account for the difference in
390 the TER, E-cadherin, claudin-2, and cytokine response of colon tumor cell lines and primary
391 human colon organoids. First, as noted above, the effects of BFT-2 are dose dependent [18].
392 OMVs secreted by ETBF and NTBF+*bft* contain endogenous levels of BFT-2. It is possible that
393 the concentration of recombinant BFT-2 in previous studies was much higher than the amount
394 of native BFT-2 in OMVs, although a comparison of concentrations is not possible given
395 available data. Second, the duration of exposure to OMVs may be a factor. The literature
396 reports that the effects of recombinant BFT-2 on E-cadherin and claudin-2 in cell lines required
397 anywhere from 1 hr. to several hrs. of exposure[3,9,10]. Our study was limited to a one-hr.
398 exposure, which has been long enough to produce significant effects in many previous studies
399 with recombinant BFT-2 and colon cell lines [3,9,10].

400 There are a few other reports describing the development of monolayers of epithelial cells
401 derived from healthy colon organoids [31,32]. Sen et al. [32] reported that the gene expression profile
402 of human colon organoids was significantly different from the Caco-2 cell line, an immortalized
403 cell line of human colorectal adenocarcinoma cells, which had a gene expression profile similar
404 to the small intestine. They reported that the effect of *Bifidobacterium longum* on gene
405 expression was not conserved between Caco-2 and colon organoids. Taglieri et al [31] reviewed
406 the literature on human colon organoids and noted that air liquid interface culture increased
407 differentiation of colon organoids. However, none of the other studies on colon organoids
408 exposed them to OMVs or reported CFTR Cl^- secretion.

409 OMVs secreted by most strains of *B. fragilis* in the present study inhibited forskolin-stimulated
410 CFTR Cl^- secretion by the proximal colon and T84 cells, which would reduce salt and fluid
411 secretion by the colon. However, studies in animals report that recombinant BFT-2 induces

412 secretory diarrhea [3,6-8]. One possible reason for the different effects of recombinant BFT-2 and
413 OMVs containing BFT-2 is that the effect of BFT-2 is dose dependent, and that recombinant
414 BFT-2 levels in published studies may be higher than the abundance of BFT-2 in OMVs. As
415 demonstrated in Figure 3 and the Supplemental Tables, OMVs contain many proteins in
416 addition to BFT-2, which may influence CFTR Cl^- secretion by primary human colon organoids.
417 Finally, it is important to note that there are other pathways that mediate transepithelial salt and
418 water transport by the proximal colon, including electroneutral NaCl and fluid reabsorption
419 mediated by the parallel operation of Na^+/H^+ and Cl^-/HCO_3^- (SLC26A3) exchangers. Since
420 Ussing chamber studies only measure electrogenic transport, it is possible that recombinant
421 BFT-2 (and endogenous BFT-2) may inhibit SLC26A3 and/or the Na^+/H^+ exchanger *in vivo* and
422 thereby reduce electroneutral NaCl and fluid reabsorption by the colon. Such an effect may
423 contribute to the ETBF-induced secretory diarrhea, despite the OMV reduction in electrogenic
424 CFTR Cl^- secretion reported herein. Thus, extensive additional studies, beyond the goals of the
425 present study, are required to determine if BFT-2 and OMVs inhibit Na^+/H^+ and Cl^-/HCO_3^-
426 electrically neutral NaCl and fluid reabsorption in primary human colon organoids. Such studies
427 would require use of radioactive isotopes and chemical inhibitors of electrically neutral
428 transporters and/or antisense experiments to selectively reduce electroneutral transporter
429 expression.

430 We also did not observe an effect of any OMVs on the TER or epithelial tight junction or cell
431 adhesion structure. In many, but not all, previous studies in colon cell lines, recombinant BFT-2
432 quickly (< 1 hr.) reduced the abundance of E-cadherin and the TER [9,15,17,19,20]. Although the
433 reason for this difference is unknown, one possible explanation for the different effects of
434 recombinant BFT-2 and OMVs is that, as noted above, the effect of recombinant BFT-2 is dose
435 and time dependent, and that recombinant BFT-2 levels in published studies may be higher
436 than the abundance of endogenous BFT-2 in in OMVs.

437 In contrast to studies using cells lines and recombinant BFT-2 [10,48-50], we did not observe a
438 significant increase in IL-8 secretion in primary human colon organoids exposed to OMVs. The
439 lack of effect of BFT-2 and OMVs on IL-8 secretion in our study are consistent with the
440 observation that OMVs did not reduce E-cadherin, an effect reported to be required for BFT-2 to
441 stimulate IL-8 secretion [10,48-50]. OMVs did not affect the secretion of any of the 48 cytokines as
442 determined by the MILLIPLEX MAP Human Cytokine/Chemokine 48-Plex cytokine assay. The
443 reason for this difference is also unknown and requires additional studies.

444 There are a few limitations of our study. First, since there are many differences in the content of
445 OMVs secreted by ETBF and NTBF such as DNA, RNA, miRNA, proteins (this study) and other
446 virulence factors [24,51], in addition to BFT-2, it is possible that some of these factors may act
447 alone of in concert with BFT-2 to inhibit CFTR Cl^- secretion. Second, although we did not
448 complement the *bft-2* gene in ETBF Δ*bft*, due in part to the technical challenge of
449 complementation in our clinical strain, we have complementary lines of evidence to support our
450 conclusions that BFT-2 inhibits CFTR Cl^- secretion in colon organoids. First, we utilized two
451 strains o*f B. fragilis* that lack BFT-2 (ETBF Δ*bft* and NTBF) and two that secrete BFT-2 (ETBF
452 and NTBF+*bft*). Our results on primary human colon organoids are similar in ETBF Δ*bft* and
453 NTBF, as are the results using ETBF and NTBF+*bft*.

454 Our study has numerous strengths. First, our experiments were conducted on well differented
455 human colon organoids from three healthy donors, and a cell line (T84). OMVs inhibited CFTR
456 Cl^- secretion by colon organoids and T84 cells, but had no effect on TER, or the expression of
457 claudin-2 and E-cadherin. Second since *B. fragilis* resides in mucus overlying colon organoids,
458 OMVs containing BFT-2 are biologically relevant. Notably, the concentration of OMVs used in
459 the present study was similar to levels observed in conditioned cell culture media and biological
460 fluids[21,39], and the same number of OMVs was used in all experimental groups [21,39].

461 In conclusion, we have examined the effects of OMVs on well differentiated primary cultures of
462 human colon organoids secreted by *B. fragilis* containing *bft-2 (*ETBF and NTBF+*bft)*, a strain of
463 *B. fragilis* in which *bft-2* was knocked out (ETBF Δ*bft*), and an NTBF strain that does not
464 express *bft-2.* In all cases, BFT-2 containing OMVs secreted by *B. fragilis* reduced forskolin-
465 stimulated CFTR Cl^- secretion by colon organoids more than the same strain lacking *bft-2* but
466 had no effect on tight junction structure (E-cadherin and claudin-2), TER, amiloride-sensitive
467 sodium absorption, or IL-8 secretion. Similar experiments on the T84 cell line also revealed that
468 OMVs secreted by *B. fragilis* reduced CFTR Cl^- secretion and had no effect on TER. We
469 conclude that *B. fragilis* OMVs containing biologically significant levels of BFT-2 inhibit forskolin
470 stimulated CFTR Cl^- secretion by primary human colon organoids, without effecting TER,
471 amiloride-sensitive Na^+ currents and cytokine secretion. Additional studies, beyond the scope of
472 the present study, are required to elucidate the cellular mechanisms whereby OMVs rapidly
473 inhibit CFTR Cl^- secretion. Although the results in this study contradict many studies using cell
474 lines and recombinant BFT-2, we anticipate that our results will stimulate a discussion of the
475 effects on BFT-2 on the colon.

476 **METHODS**

477 **Bacteroides culture and genetics**. *B. fragilis* NCTC 9343 was chosen as the non-toxigenic *B.*
478 *fragilis* (NTBF) strain, since it is used widely [52-54]. *B. fragilis* 86-5443-2-2 was chosen as the
479 enterotoxigenic *B. fragilis* (ETBF) strain for similar reasons, and because it expresses BFT-2,
480 which is the most virulent of the three BFT isotypes [52-54]. *B. fragilis* 86-5443-2-2 with a *bft*
481 deletion (ETBF Δ*bft*), provided by Dr. Cynthis Sears, was confirmed by PCR [55]. To construct the
482 NTBF+*bft* strain, we first PCR amplified *bft-2* from *B. fragilis* 86-5443-2-2 and cloned it via
483 Gibson Assembly into the SalI and NcoI sites of the *Bacteroides* expression plasmid pNBU2-
484 P1T-DP-A21 [56]. This plasmid integrates in single copy into the chromosomal att sites of
485 *Bacteroides fragilis.* The sequence of the resulting plasmid was confirmed by Sanger

486 sequencing before transformation into *E. coli* S17-1 cells and conjugation via overnight aerobic
487 solid agar co-culture mating into *B. fragilis* 9343 (NTBF). Following incubation, matings were
488 resuspended and plated on BHIS agar containing gentamycin and erythromycin. Att
489 chromosomal integration site was confirmed by PCR [57]. Bacteroides strains were grown on
490 supplemented brain heart infusion medium (BHIS) agar plates or liquid broth cultures
491 supplemented with hemin and 1μg/ml of vitamin K3 (Acros Organics/Fisher Scientific, Geel,
492 Belgium) under anaerobic conditions (10% CO_2, 10% H_2, 80% N_2) in a Whitley A55 anaerobic
493 chamber (Don Whitley Scientific, Victoria Works, UK) at 37°C. All BHIS agar and liquid media
494 contained 60 μg/ml of gentamycin sulfate. For OMV purification, *B. fragilis* strains were streaked
495 on BHIS agar plates and were grown in anaerobic conditions for 48 hrs. Single colonies were
496 used to inoculate 5mL of BHIS liquid medium cultures, which were grown anaerobically for 24
497 hrs. The cultures were then expanded into 200mL BHIS cultures using a 1:100 dilution. The final
498 cultures were grown for 24 hrs. prior to being utilized to isolate OMVs.

499 **Outer membrane vesicle (OMV) isolation.** OMVs were isolated as described by us and others
500 previously [23,58]. Briefly, all overnight culture supernatants were centrifuged for 1 hr. at 2800 g
501 and 4°C to pellet bacteria. The supernatant was filtered twice through 0.45 μm PVDF
502 membrane filters (Millipore, Billerica, MA, USA) to remove any contaminating bacteria and
503 concentrated with 30K Amicon filters (Millipore, Billerica, MA, USA) at 2800 g and 4°C to obtain
504 ~200μL of concentrate. The concentrate was resuspended in OMV buffer (20 mM HEPES, 500
505 mM NaCl, pH 7.4) and subjected to ultracentrifugation using a TH-660 Swinging Bucket rotor
506 (Thermo Fisher) for 2 hrs. at 200,000 g and 4°C to pellet OMVs. OMV pellets were then re-
507 suspended in 60% OptiPrep Density Gradient Medium (Sigma-Aldrich, Cat. # D1556) and
508 layered with 35%, 30% and 20% OptiPrep diluted in OMV buffer. OMVs in OptiPrep were
509 centrifuged for 18 hrs. at 100,000 g and 4°C. 500μl fractions were taken from the top of the
510 gradient, with OMVs residing in fractions 5-8, as determined by proteomic analysis of OMVs.

511 **Electron microscopy of OMVs**. OMVs were visualized with negative staining transmission
512 electron microscopy as described previously [22]. The microscopist was blinded to the
513 experimental treatment to minimize observer bias. Briefly, an aliquot of each sample was
514 applied onto a freshly glow-discharged 200-mesh nickel grid and allowed to sit for two minutes.
515 After incubation, excess fluid was gently removed with filter paper, and the grids were
516 sequentially rinsed with Millipore-filtered distilled water. While the grids remained slightly damp,
517 they were placed onto a drop of Nano-W tungsten stain (Ted Pella, Inc.). Excess stain was
518 absorbed with filter paper, and the staining step was repeated on a second drop of Nano-W,
519 which was allowed to sit for one minute before being wicked away and left to dry. Imaging of the
520 stained grids was conducted at 80 kV on a JEOL 1400 transmission electron microscope (JEOL
521 USA Inc.), and images were captured using an AMT XR11 digital camera (AMT).

522 **Proteomics characterization of OMVs.** To confirm that BFT-2 was secreted by ETBF and
523 NTBF+*bft* in OMVs, but not by ETBF Δ*bft* and NTBF OMVs, OMVs were isolated as described
524 above and pelleted and lysed in buffer containing 0.5%SDS, 50mM ammonium bicarbonate,
525 50mM NaCl, and Halt Protease Inhibitor. Mass spectrometry analysis was performed by the
526 Mass Spectrometry Technology Access Center (MTAC) at Washington University School of
527 Medicine using previously published protocols [59]. Samples were purified by trichloroacetic acid
528 precipitation. After pelleting and washing with ice-cold acetone, the resulting protein pellet was
529 resuspended in 8M urea and 0.4M ammonium bicarbonate, reduced with 4mM dithiothreitol,
530 and alkylated with 18mM iodoacetamide. The solution was then diluted to <2M urea, and 1µg of
531 trypsin was added for overnight digestion at 37°C. The resulting peptides were desalted using
532 C18 solid-phase extraction spin columns, and eluates were dried under vacuum using a
533 SpeedVac concentrator. Peptides were analyzed by LC–MS/MS using a nanoElute2 coupled to
534 a timsTOF Pro2 mass spectrometer (Bruker Daltonics). Samples were separated on a C18
535 column (150µm × 25cm, 1.5µm; Bruker). The mobile phases consisted of 0.1% formic acid (FA)

536 in water (mobile phase A) and 0.1%FA in acetonitrile (mobile phase B). Peptides were
537 separated using a 54-min. linear gradient from 3% to 35% mobile phase B, with a total run time
538 of 60 mins. at a constant flow rate of 600nL/min. The timsTOF Pro2 was operated in dia-PASEF
539 mode. Spectra were acquired across an m/z range of 300-1200, using 28 mass windows per
540 cycle. The inverse reduced ion mobility ($1/K_0$) range was set to 0.65–1.35 V·s/cm². The trapped
541 ion mobility spectrometry (TIMS) analyzer operated at a 100% duty cycle with a ramp time of 75
542 ms., yielding an overall cycle time of approximately 1.20 seconds. Collision energy was linearly
543 ramped from 59 eV at $1/K_0$ = 1.6 to 20 eV at $1/K_0$ = 0.6. dia-PASEF data files were analyzed
544 using directDIA™ workflow embedded in Spectronaut 18 (Biognosys AG) against the
545 *Bacteroides fragilis* database. Search parameters included trypsin digestion with cleavage after
546 K or R, allowance for up to two missed cleavages, carbamidomethylation of cysteine (static
547 modification), and variable modifications including oxidized methionine and Protein N-terminal
548 acetylation. Peptide spectrum matches (PSMs), peptides, and protein groups were identified
549 using a false discovery rate (FDR) threshold of 0.01. For quantification, all fragment ions
550 passing the FDR threshold were used, and protein abundances were calculated as the area
551 under the curve of extracted ion chromatograms within the defined peak boundaries for each
552 targeted ion. The mass spectrometry proteomics data have been deposited to the
553 ProteomeXchange Consortium via the PRIDE partner repository[60] with the dataset identifier
554 PXD073462.

555 **Colon organoid cell culture.** Biopsies from the proximal colon obtained during colonoscopies
556 of three healthy de-identified donors were obtained after informed consent at Dartmouth-Health.
557 Biopsies in PBS (-/-) with EDTA were placed on a shaking rocker in +4°C for 1 hr. to free the
558 crypts from the biopsies. Then the biopsies were vigorously pipetted up and down several times
559 to release crypts. The supernatant containing crypts was collected, and additional PBS was
560 added to the biopsies followed by vigorous pipetting. Crypts in the supernatant were counted,

561 pelleted, and resuspended in 55% Matrigel (Corning Life Sciences) and 45% isolation medium.
562 Cells were added to 24-well plates and then Matrigel solidified cell isolation medium (IntestiCult
563 complete medium with primocin [StemCell Technologies] supplemented with 50ug/mL
564 gentamycin, 50ug/mL vancomycin and 10uM of RhoKi) was added to each well. Cells were
565 maintained in culture until spherical organoids were observed. To develop polarized monolayers
566 of organoids, 1.5 x 10^6 cells (as spherical organoids) were collected from the Matrigel and
567 seeded on Transwell permeable filters (#3450: Corning Life Sciences for 24-mm Transwell) or
568 12-mm Snapwell permeable filters (#3801; Corning Life Sciences). Filters were precoated with a
569 1:20 dilution of Matrigel in cold DPBS for 2 hrs. and then removed just before seeding cells.
570 IntestiCult media (StemCell Technologies) was added to both apical and basolateral sides of the
571 filters to support cell growth. Once a confluent monolayer was obtained, IntestiCult
572 differentiation media (StemCell Technologies) was used to differentiate the cells prior to
573 experimentation. Cells were differentiated for one week before experiments.

574 **Exposure of primary human colon organoids to OMVs.** Polarized monolayers of colon
575 organoids on 12-mm Snapwell filters were washed with PBS to remove excess mucus, and 1.5
576 mL of differentiation media was added to the basolateral side. 2 × 10^{10} OMVs from all strains of
577 *B. fragilis*, a concentration of OMVs similar to that measured in conditioned media and in
578 biological fluids [21,39], or the same volume of process control (PC) media were applied to the
579 apical side of cells for 1 hr. and then removed. At the end of the 1hr. exposure and then 24 hrs.
580 later the apical and basolateral media were collected for measurements of cytokines
581 [MILLIPLEX MAP Human Cytokine/Chemokine 48-Plex cytokine assay (MilliporeSigma)].
582 Ussing chamber analysis was used to quantify CFTR Cl^- secretion, sodium absorption and TER
583 as described [61,62].

584 **T84 cell culture**. T84 cells, a human colon adenocarcinoma cell line (American Type Culture
585 Collection, Manassas, VA) were maintained in DMEM/F-12 media (ATCC) containing l-

586 glutamine supplemented with 5% fetal bovine serum (FBS: Life Technology). For short-circuit
587 current and TER measurements cells were cultured on Transwell filters (Corning, Ithaca, NY).
588 Experiments were performed 21 days postseeding as previously described [40-42].

589 **Ussing chamber measurements of sodium and CFTR Cl^- currents.** As described in detail
590 elsewhere [63-66] cells on Snapwell or Transwell filters were mounted in Ussing chambers. Primary
591 human colon organoids and T84 cells were exposed to either process control (PC: BHIS growth
592 media processed through the OMV isolation procedure, as a control for possible effects on
593 colon organoids due to the media or the OMV isolation process as recommended by the
594 International Society of Extracellular Vesicles [67]) or OMVs secreted by ETBF, ETBF Δ*bft*, NTBF,
595 or NTBF+*bft* were added to the apical side of monolayers for 1 hr. then CFTR Cl^- currents,
596 amiloride-sensitive sodium currents (in colon organoids only since T84 cells do display
597 amiloride-sensitive sodium currents) and TER were measured. Some monolayers were exposed
598 to OMVs for 1 hr., followed by washing OMVs from the apical surface and 24 hrs. later CFTR
599 Cl^- currents and TER were measured. To measure TER, a 1 mV pulse was applied to each
600 monolayer and the change in short circuit current was measured and TER was calculated using
601 Ohms Law. Electrogenic sodium currents were reported as amiloride-sensitive currents, since
602 amiloride inhibits the epithelial sodium channel ENaC [68]. To measure CFTR Cl^- secretion,
603 amiloride (50 μM) was first added to the apical solution to inhibit and measure sodium
604 reabsorption. Thereafter, Cl^- secretion was stimulated with forskolin (10 μM; Sigma-Aldrich),
605 which increases protein kinase A that phosphorylates and activates CFTR Cl^- secretion [38].
606 Finally, thiazolidinone ($CFTR_{inh}$-172, 20 μM; Millipore, Billerica, MA), an inhibitor of CFTR Cl^-
607 channels, was added to the apical solution [64]. Data are expressed as the forskolin-stimulated,
608 $CFTR_{inh}$-172 inhibited short circuit current (Isc), which is presented as $\mu A/cm^2$. Data were
609 collected and analyzed using the Data Acquisition Software Acquire and Analyze program
610 (Physiologic Instruments, San Diego, CA).

611 **Cytokine measurements.** Cytokine secretion (apical and basolateral solutions) from primary
612 human colon organoids was measured with the MILLIPLEX MAP Human Cytokine/Chemokine
613 48-Plex cytokine assay (MilliporeSigma) following the manufactures instructions.

614 **Immunocytochemistry.** Immunocytochemistry was performed to characterize cell types in the
615 colon organoids and to evaluate the effects of OMVs on E-cadherin and claudin-2. Fixation of
616 colon organoids was performed using 4% paraformaldehyde for 15 mins. at room temperature,
617 followed by permeabilization with 0.25% Triton X-100 for 15 mins., blocking using 10% normal
618 goat serum in PBS, and primary antibody incubation at 4°C overnight. After washing, secondary
619 antibodies were added for 1 hr. at room temperature in the dark. SLC26A3 was labeled with a
620 primary anti-mouse antibody (1:250, Santa Cruz #sc-376187), and a secondary goat anti-
621 mouse-488 antibody (1:500, Santa Cruz #sc-376187). CFTR was labeled with a primary anti-
622 mouse antibody (1:100, Millipore # 05-583) and a secondary anti-mouse-488 antibody (1:500).
623 MUC2 was labeled with a primary anti-mouse antibody (1:300), and a secondary anti-mouse-
624 488 antibody (1:500, Abcam ab11197). Chromogranin A was labeled with a primary goat anti
625 rabbit antibody (1:100), and secondary goat anti rabbit-568 antibody (1:1000, Abcam ab15760).
626 Tight junction labeling was performed by fixing cells in 100% cold methanol at -20°C for 5 mins.,
627 blocking with 10% goat serum in PBS for 1 hr., and incubating with primary antibodies at 4°C
628 overnight. The secondary antibody was added for 1 hr. at room temperature the following day.
629 Claudin-2 was labeled using a primary goat anti-rabbit antibody (1:100, Thermo Fisher #51-
630 6100), and a secondary goat anti-rabbit-568 antibody (1:500). E-cadherin was labeled using a
631 primary goat anti-mouse antibody (1:250, BD Transduction lab #610182), and a secondary goat
632 anti-mouse-488 antibody (1:500). All antibodies were diluted in PBS with 5% normal goat
633 serum. DAPI staining to label nuclei was performed in fluorshield anti-fade mounting medium.
634 To image the colon organoids, a Yokogawa W1 spinning disk unit coupled to a Nikon Ti-E
635 inverted microscope was used. To examine the effect of OMVs and PC on claudin-2 and E-

636 cadherin, all settings on the confocal microscope were identical for acquiring images for
637 analysis. Analysis of claudin-2 and E-cadherin abundance was performed by an investigator
638 blinded to the treatments. The membrane areas with positive fluorescence signal were
639 segmented using trainable WEKA machine learning plugin in ImageJ [69]. The segmented objects
640 were thinned to 1 pixel using ImageJ's "Skeletonize" morphological operation. The mean and
641 median fluorescence intensities were measured from areas defined by the skeleton and
642 widened to 5 pixels using ImageJ's "Dilate" morphological operation.

643 **Statistics.** Data were analyzed using the R software environment for statistical computing and
644 graphics version 4.1.0 [70] , Ingenuity Pathway Analysis and Prism (GraphPad). Statistical
645 significance was calculated using either a mixed effect linear model, or likelihood ratio tests on
646 gene-wise negative binomial generalized linear models, as indicated in the figure legends. Data
647 were visualized, and figures were created using Prism or ggplot.

648 **Author contributions**

649 PS, RB, AN, BAS, CR, TTH and BR designed the research studies. PS, RB, AN, CR, TTH and
650 ZS conducted experiments on human colon organoids and T84 cells, acquired data, and
651 analyzed data. TBG recruited human subjects, provided informed consent and collected clinical
652 biopsies. YAG and BKC performed the proteomics analysis of OMVs. Electron microscopy of
653 OMVs was performed by DJT and Brad Vietje at the Microscopy Imaging Center at the
654 University of Vermont (RRID# SCR_018821). BAS wrote the first and revised draft of the
655 manuscript. All authors contributed to the article and approved the submitted version.

656 **Declaration of competing interests**

657 All authors declare no competing interests.

658 **IRB statement**

659 The Dartmouth Committee for the Protection of Human Subjects has determined that using
660 colon biopsies in this study is not considered human subject research because they contain no
661 patient identifiers. All tissues used for isolation were obtained under informed consent and
662 conform to HIPAA regulations to protect the privacy of the donor's personally identifiable
663 information.

664 **Data availability.** The mass spectrometry proteomics data are available in the Supplemental
665 Tables and have been deposited to the ProteomeXchange Consortium via the PRIDE partner
666 repository[60] with the dataset identifier PXD073462. All other reasonable requests for additional
667 data are available from the corresponding author.

668 **Funding Declaration**. This study was supported by the Cystic Fibrosis Foundation
669 (STANTO19G0, STANTO20P0, STANTO23R0, and STANTO19R0) and the National Institutes
670 of Health [P30-DK117469 (Pilot Project Award) and R01HL151385] to BAS. BDR was
671 supported by NIH R35GM142685 and CFF ROSS20R3 and is the Phil Hanlon First Century
672 Associate Professor in Personalized Treatment for Cystic Fibrosis. PS was supported by T32-
673 HL134598. Electron Microscopy was performed at the Microscopy Imaging Center, Larner
674 College of Medicine, University of Vermont (RRID# SCR_01882). Mass Spectrometry analyses
675 were performed by the Mass Spectrometry Technology Access Center at the McDonnell
676 Genome Institute (MTAC@MGI) at Washington University School of Medicine, supported by the
677 Diabetes Research Center/NIH grant P30 DK020579, Institute of Clinical and Translational
678 Sciences/NCATS CTSA award UL1 TR002345, and Siteman Cancer Center/NCI CCSG grant
679 P30 CA091842. We thank Dr. Samuel Smukowski (Washington University School of Medicine)
680 for his support and advice on the mass spectrometry analyses.

681

682 **Acknowledgements.** Cynthia Sears, M.D. (Johns Hopkins University) generously provided the
683 ETBF Δ*bft* strain. Scott Palisoul (Dartmouth Pathology Shared Resources) created frozen cross
684 sections of 2D colon organoids. We thank Brad Vietje for the electron micrograph's and Katja
685 Koeppen, Ph.D. for analysis of the T84 data.

686 **SUPPLEMENTAL TABLES**

687 **Supplemental Table 1.** Mass spectrometry quantification of proteins detected exclusively in *B.*
688 *fragilis* NTBF OMVs.

689 **Supplemental Table 2.** Mass spectrometry quantification of proteins detected exclusively in *B.*
690 *fragilis* ETBF OMVs.

691 **Supplemental Table 3.** Mass spectrometry quantification of proteins detected in both *B. fragilis*
692 NTBF and *B. fragilis* ETBF OMVs.

693 **Supplemental Table 4.** Differential expression results of proteins identified in mass
694 spectrometry for both *B. fragilis* ETBF and *B. fragilis* NTBF

695 **References**

696 1 Jasemi, S. *et al.* Biological Mechanisms of Enterotoxigenic Bacteroides fragilis Toxin:
697 Linking Inflammation, Colorectal Cancer, and Clinical Implications. *Toxins (Basel)* **17**
698 (2025). https://doi.org/10.3390/toxins17060305
699 2 Ferranti, E. P., Dunbar, S. B., Dunlop, A. L. & Corwin, E. J. 20 things you didn't know
700 about the human gut microbiome. *J Cardiovasc Nurs* **29**, 479-481 (2014).
701 https://doi.org/10.1097/JCN.0000000000000166
702 3 Valguarnera, E. & Wardenburg, J. B. Good Gone Bad: One Toxin Away From Disease
703 for Bacteroides fragilis. *J Mol Biol* **432**, 765-785 (2020).
704 https://doi.org/10.1016/j.jmb.2019.12.003

705 4 Human Microbiome Project, C. Structure, function and diversity of the healthy human
706 microbiome. *Nature* **486**, 207-214 (2012). https://doi.org/10.1038/nature11234
707 5 Young, V. B. The role of the microbiome in human health and disease: an introduction
708 for clinicians. *BMJ* **356**, j831 (2017). https://doi.org/10.1136/bmj.j831
709 6 Saha, K., Zhou, Y. & Turner, J. R. Tight junction regulation, intestinal permeability, and
710 mucosal immunity in gastrointestinal health and disease. *Curr Opin Gastroenterol* **41**,
711 46-53 (2025). https://doi.org/10.1097/MOG.0000000000001066
712 7 Hill, C. A. *et al.* Bacteroides fragilis toxin expression enables lamina propria niche
713 acquisition in the developing mouse gut. *Nat Microbiol* **9**, 85-94 (2024).
714 https://doi.org/10.1038/s41564-023-01559-9
715 8 Sears, C. L. *et al.* Association of enterotoxigenic Bacteroides fragilis infection with
716 inflammatory diarrhea. *Clin Infect Dis* **47**, 797-803 (2008).
717 https://doi.org/10.1086/591130
718 9 Kim, W. S. *et al.* Bacteroides fragilis Toxin Induces Sequential Proteolysis of E-Cadherin
719 and Inflammatory Response in Mouse Intestinal Epithelial Cell Line. *Microorganisms* **13**
720 (2025). https://doi.org/10.3390/microorganisms13040781
721 10 Hwang, S., Gwon, S. Y., Kim, M. S., Lee, S. & Rhee, K. J. Bacteroides fragilis Toxin
722 Induces IL-8 Secretion in HT29/C1 Cells through Disruption of E-cadherin Junctions.
723 *Immune Netw* **13**, 213-217 (2013). https://doi.org/10.4110/in.2013.13.5.213
724 11 Guo, Y. *et al.* Mechanistic diversity of Bacteroides fragilis toxins and neutralization with
725 single domain antibody. *Cell Chem Biol* **33**, 102-116 e106 (2026).
726 https://doi.org/10.1016/j.chembiol.2025.12.009
727 12 Zakharzhevskaya, N. B. *et al.* Interaction of Bacteroides fragilis Toxin with Outer
728 Membrane Vesicles Reveals New Mechanism of Its Secretion and Delivery. *Front Cell*
729 *Infect Microbiol* **7**, 2 (2017). https://doi.org/10.3389/fcimb.2017.00002

730 13 Rong, Y. *et al.* Partially differentiated ileal and distal-colonic human F508del-cystic
731 fibrosis-enteroids secrete fluid in response to forskolin and linaclotide. *iScience* **28**,
732 112453 (2025). https://doi.org/10.1016/j.isci.2025.112453
733 14 Negussie, A. B., Dell, A. C., Davis, B. A. & Geibel, J. P. Colonic Fluid and Electrolyte
734 Transport 2022: An Update. *Cells* **11** (2022). https://doi.org/10.3390/cells11101712
735 15 Riegler, M. *et al.* Bacteroides fragilis toxin 2 damages human colonic mucosa in vitro.
736 *Gut* **44**, 504-510 (1999). https://doi.org/10.1136/gut.44.4.504
737 16 Obiso, R. J., Jr., Azghani, A. O. & Wilkins, T. D. The Bacteroides fragilis toxin fragilysin
738 disrupts the paracellular barrier of epithelial cells. *Infect Immun* **65**, 1431-1439 (1997).
739 https://doi.org/10.1128/iai.65.4.1431-1439.1997
740 17 Wu, S., Rhee, K. J., Zhang, M., Franco, A. & Sears, C. L. Bacteroides fragilis toxin
741 stimulates intestinal epithelial cell shedding and gamma-secretase-dependent E-
742 cadherin cleavage. *J Cell Sci* **120**, 1944-1952 (2007). https://doi.org/10.1242/jcs.03455
743 18 Sheikh, A. *et al.* Outer membrane vesicles from Bacteroides fragilis contain coding and
744 non-coding small RNA species that modulate inflammatory signaling in intestinal
745 epithelial cells. *bioRxiv* (2025). https://doi.org/10.1101/2025.06.25.661399
746 19 Kharlampieva, D. D. *et al.* Purification and characterisation of recombinant Bacteroides
747 fragilis toxin-2. *Biochimie* **95**, 2123-2131 (2013).
748 https://doi.org/10.1016/j.biochi.2013.08.005
749 20 Chambers, F. G. *et al.* Bacteroides fragilis toxin exhibits polar activity on monolayers of
750 human intestinal epithelial cells (T84 cells) in vitro. *Infect Immun* **65**, 3561-3570 (1997).
751 https://doi.org/10.1128/iai.65.9.3561-3570.1997
752 21 Charpentier, L. A. *et al.* Bacterial Outer Membrane Vesicles and Immune Modulation of
753 the Host. *Membranes (Basel)* **13** (2023). https://doi.org/10.3390/membranes13090752

754 22 Li, Z. *et al.* P. aeruginosa tRNA-fMet halves secreted in outer membrane vesicles
755 suppress lung inflammation in cystic fibrosis. *Am J Physiol Lung Cell Mol Physiol* **326**,
756 L574-L588 (2024). https://doi.org/10.1152/ajplung.00018.2024
757 23 Koeppen, K. *et al.* A Novel Mechanism of Host-Pathogen Interaction through sRNA in
758 Bacterial Outer Membrane Vesicles. *PLoS Pathog* **12**, e1005672 (2016).
759 https://doi.org/10.1371/journal.ppat.1005672
760 24 Yang, Y. *et al.* Bacteroides Fragilis-Derived Outer Membrane Vesicles Deliver MiR-5119
761 and Alleviate Colitis by Targeting PD-L1 to Inhibit GSDMD-Mediated Neutrophil
762 Extracellular Trap Formation. *Adv Sci (Weinh)*, e00781 (2025).
763 https://doi.org/10.1002/advs.202500781
764 25 Shagaleeva, O. Y. *et al.* Bacteroides vesicles promote functional alterations in the gut
765 microbiota composition. *Microbiol Spectr* **12**, e0063624 (2024).
766 https://doi.org/10.1128/spectrum.00636-24
767 26 Patrick, S., McKenna, J. P., O'Hagan, S. & Dermott, E. A comparison of the
768 haemagglutinating and enzymic activities of Bacteroides fragilis whole cells and outer
769 membrane vesicles. *Microb Pathog* **20**, 191-202 (1996).
770 https://doi.org/10.1006/mpat.1996.0018
771 27 Sharpe, S. W., Kuehn, M. J. & Mason, K. M. Elicitation of epithelial cell-derived immune
772 effectors by outer membrane vesicles of nontypeable Haemophilus influenzae. *Infect*
773 *Immun* **79**, 4361-4369 (2011). https://doi.org/10.1128/IAI.05332-11
774 28 Round, J. L. *et al.* The Toll-like receptor 2 pathway establishes colonization by a
775 commensal of the human microbiota. *Science* **332**, 974-977 (2011).
776 https://doi.org/10.1126/science.1206095
777 29 Lee, S. M. *et al.* Bacterial colonization factors control specificity and stability of the gut
778 microbiota. *Nature* **501**, 426-429 (2013). https://doi.org/10.1038/nature12447

779 30 Sears, C. L., Geis, A. L. & Housseau, F. Bacteroides fragilis subverts mucosal biology:
780 from symbiont to colon carcinogenesis. *J Clin Invest* **124**, 4166-4172 (2014).
781 https://doi.org/10.1172/JCI72334
782 31 Taglieri, M. *et al.* Colorectal Organoids: Models, Imaging, Omics, Therapy, Immunology,
783 and Ethics. *Cells* **14** (2025). https://doi.org/10.3390/cells14060457
784 32 Sen, A. *et al.* Comprehensive gene expression analysis of organoid-derived healthy
785 human colonic epithelium and cancer cell line stimulated with live probiotic bacteria. *Sci*
786 *Rep* **15**, 22325 (2025). https://doi.org/10.1038/s41598-025-07391-x
787 33 Rikkert, L. G., Nieuwland, R., Terstappen, L. & Coumans, F. A. W. Quality of
788 extracellular vesicle images by transmission electron microscopy is operator and
789 protocol dependent. *J Extracell Vesicles* **8**, 1555419 (2019).
790 https://doi.org/10.1080/20013078.2018.1555419
791 34 Noble, J. M. *et al.* Direct comparison of optical and electron microscopy methods for
792 structural characterization of extracellular vesicles. *J Struct Biol* **210**, 107474 (2020).
793 https://doi.org/10.1016/j.jsb.2020.107474
794 35 Weiss, A. *et al.* Transmission Electron Microscopy-based characterization of
795 Extracellular Vesicles from plasma and serum from Parkinson s Disease patients. *Cell*
796 *Commun Signal* **23**, 395 (2025). https://doi.org/10.1186/s12964-025-02383-w
797 36 Zakharzhevskaya, N. B. *et al.* Outer membrane vesicles secreted by pathogenic and
798 nonpathogenic Bacteroides fragilis represent different metabolic activities. *Sci Rep* **7**,
799 5008 (2017). https://doi.org/10.1038/s41598-017-05264-6
800 37 Parikh, K. *et al.* Colonic epithelial cell diversity in health and inflammatory bowel disease.
801 *Nature* **567**, 49-55 (2019). https://doi.org/10.1038/s41586-019-0992-y
802 38 Ghigo, A., De Santi, C., Hart, M., Mitash, N. & Swiatecka-Urban, A. Cell signaling and
803 regulation of CFTR expression in cystic fibrosis cells in the era of high efficiency

804 modulator therapy. *J Cyst Fibros* **22 Suppl 1**, S12-S16 (2023).
805 https://doi.org/10.1016/j.jcf.2022.12.015
806 39 Stanton, B. A. Extracellular Vesicles and Host-Pathogen Interactions: A Review of Inter-
807 Kingdom Signaling by Small Noncoding RNA. *Genes (Basel)* **12** (2021).
808 https://doi.org/10.3390/genes12071010
809 40 Howe, K. L., Wang, A., Hunter, M. M., Stanton, B. A. & McKay, D. M. TGFbeta down-
810 regulation of the CFTR: a means to limit epithelial chloride secretion. *Exp Cell Res* **298**,
811 473-484 (2004). https://doi.org/10.1016/j.yexcr.2004.04.026
812 41 Maitra, R., Shaw, C. M., Stanton, B. A. & Hamilton, J. W. Increased functional cell
813 surface expression of CFTR and DeltaF508-CFTR by the anthracycline doxorubicin. *Am*
814 *J Physiol Cell Physiol* **280**, C1031-1037 (2001).
815 https://doi.org/10.1152/ajpcell.2001.280.5.C1031
816 42 Maitra, R., Shaw, C. M., Stanton, B. A. & Hamilton, J. W. Functional enhancement of
817 CFTR expression by mitomycin C. *Cell Physiol Biochem* **11**, 93-98 (2001).
818 https://doi.org/10.1159/000047796
819 43 Pierce, J. V., Fellows, J. D., Anderson, D. E. & Bernstein, H. D. A clostripain-like
820 protease plays a major role in generating the secretome of enterotoxigenic Bacteroides
821 fragilis. *Mol Microbiol* **115**, 290-304 (2021). https://doi.org/10.1111/mmi.14616
822 44 Choi, V. M. *et al.* Activation of Bacteroides fragilis toxin by a novel bacterial protease
823 contributes to anaerobic sepsis in mice. *Nat Med* **22**, 563-567 (2016).
824 https://doi.org/10.1038/nm.4077
825 45 Elhenawy, W., Debelyy, M. O. & Feldman, M. F. Preferential packing of acidic
826 glycosidases and proteases into Bacteroides outer membrane vesicles. *MBio* **5**, e00909-
827 00914 (2014). https://doi.org/10.1128/mBio.00909-14
828 46 France, M. M. & Turner, J. R. The mucosal barrier at a glance. *J Cell Sci* **130**, 307-314
829 (2017). https://doi.org/10.1242/jcs.193482

830 47 Citi, S. *et al.* A short guide to the tight junction. *J Cell Sci* **137** (2024).
831 https://doi.org/10.1242/jcs.261776
832 48 Han, Y. W. *et al.* Interactions between periodontal bacteria and human oral epithelial
833 cells: Fusobacterium nucleatum adheres to and invades epithelial cells. *Infect Immun* **68**,
834 3140-3146 (2000). https://doi.org/10.1128/IAI.68.6.3140-3146.2000
835 49 Antosca, K. M. *et al.* Altered Stool Microbiota of Infants with Cystic Fibrosis Shows a
836 Reduction in Genera Associated with Immune Programming from Birth. *J Bacteriol* **201**
837 (2019). https://doi.org/10.1128/JB.00274-19
838 50 Lee, C. G. *et al.* Bacteroides fragilis Toxin Induces Intestinal Epithelial Cell Secretion of
839 Interleukin-8 by the E-Cadherin/beta-Catenin/NF-kappaB Dependent Pathway.
840 *Biomedicines* **10** (2022). https://doi.org/10.3390/biomedicines10040827
841 51 Choi, J. W., Kim, S. C., Hong, S. H. & Lee, H. J. Secretable Small RNAs via Outer
842 Membrane Vesicles in Periodontal Pathogens. *J Dent Res* **96**, 458-466 (2017).
843 https://doi.org/10.1177/0022034516685071
844 52 Franco, A. A. The Bacteroides fragilis pathogenicity island is contained in a putative
845 novel conjugative transposon. *J Bacteriol* **186**, 6077-6092 (2004).
846 https://doi.org/10.1128/JB.186.18.6077-6092.2004
847 53 Wu, S. *et al.* A human colonic commensal promotes colon tumorigenesis via activation
848 of T helper type 17 T cell responses. *Nat Med* **15**, 1016-1022 (2009).
849 https://doi.org/10.1038/nm.2015
850 54 Chan, J. L. *et al.* Non-toxigenic Bacteroides fragilis (NTBF) administration reduces
851 bacteria-driven chronic colitis and tumor development independent of polysaccharide A.
852 *Mucosal Immunol* **12**, 164-177 (2019). https://doi.org/10.1038/s41385-018-0085-5
853 55 Chung, L. *et al.* Bacteroides fragilis Toxin Coordinates a Pro-carcinogenic Inflammatory
854 Cascade via Targeting of Colonic Epithelial Cells. *Cell Host Microbe* **23**, 203-214 e205
855 (2018). https://doi.org/10.1016/j.chom.2018.01.007

856 56 Lim, B., Zimmermann, M., Barry, N. A. & Goodman, A. L. Engineered Regulatory
857 Systems Modulate Gene Expression of Human Commensals in the Gut. *Cell* **169**, 547-
858 558 e515 (2017). https://doi.org/10.1016/j.cell.2017.03.045
859 57 Degnan, P. H., Barry, N. A., Mok, K. C., Taga, M. E. & Goodman, A. L. Human gut
860 microbes use multiple transporters to distinguish vitamin B(1)(2) analogs and compete in
861 the gut. *Cell Host Microbe* **15**, 47-57 (2014). https://doi.org/10.1016/j.chom.2013.12.007
862 58 Bauman, S. J. & Kuehn, M. J. Purification of outer membrane vesicles from
863 Pseudomonas aeruginosa and their activation of an IL-8 response. *Microbes Infect* **8**,
864 2400-2408 (2006). https://doi.org/10.1016/j.micinf.2006.05.001
865 59 Koeppen, K. *et al.* An rRNA fragment in extracellular vesicles secreted by human airway
866 epithelial cells increases the fluoroquinolone sensitivity of P. aeruginosa. *Am J Physiol*
867 *Lung Cell Mol Physiol* **325**, L54-L65 (2023). https://doi.org/10.1152/ajplung.00150.2022
868 60 Perez-Riverol, Y. *et al.* The PRIDE database at 20 years: 2025 update. *Nucleic Acids*
869 *Res* **53**, D543-D553 (2025). https://doi.org/10.1093/nar/gkae1011
870 61 Hampton, T. H., Koeppen, K., Bashor, L. & Stanton, B. A. Selection of reference genes
871 for quantitative PCR: identifying reference genes for airway epithelial cells exposed to
872 Pseudomonas aeruginosa. *Am J Physiol Lung Cell Mol Physiol* **319**, L256-L265 (2020).
873 https://doi.org/10.1152/ajplung.00158.2020
874 62 Hampton, T. H. *et al.* Gene expression responses of CF airway epithelial cells exposed
875 to elexacaftor/tezacaftor/ivacaftor (ETI) suggest benefits beyond improved CFTR
876 channel function. *Am J Physiol Lung Cell Mol Physiol.* **Dec 1;327(6):L905-L916.** (2024).
877 https://doi.org/ doi: 10.1152/ajplung.00272.2024.
878 63 Stanton, B. A., Coutermarsh, B., Barnaby, R. & Hogan, D. Pseudomonas aeruginosa
879 Reduces VX-809 Stimulated F508del-CFTR Chloride Secretion by Airway Epithelial
880 Cells. *PLoS One* **10**, e0127742 (2015). https://doi.org/10.1371/journal.pone.0127742

881 64 Barnaby, R., Koeppen, K. & Stanton, B. A. Cyclodextrins reduce the ability of
882 Pseudomonas aeruginosa outer-membrane vesicles to reduce CFTR Cl(-) secretion. *Am*
883 *J Physiol Lung Cell Mol Physiol* **316**, L206-L215 (2019).
884 https://doi.org/10.1152/ajplung.00316.2018
885 65 Talebian, L., Coutermarsh, B., Channon, J. Y. & Stanton, B. A. Corr4A and VRT325 do
886 not reduce the inflammatory response to P. aeruginosa in human cystic fibrosis airway
887 epithelial cells. *Cell Physiol Biochem* **23**, 199-204 (2009).
888 https://doi.org/10.1159/000204108
889 66 Stanton, B. A. Effects of Pseudomonas aeruginosa on CFTR chloride secretion and the
890 host immune response. *Am J Physiol Cell Physiol* **312**, C357-C366 (2017).
891 https://doi.org/10.1152/ajpcell.00373.2016
892 67 Welsh, J. A. *et al.* Minimal information for studies of extracellular vesicles (MISEV2023):
893 From basic to advanced approaches. *J Extracell Vesicles* **13**, e12404 (2024).
894 https://doi.org/10.1002/jev2.12404
895 68 Berdiev, B. K., Shlyonsky, V. G., Karlson, K. H., Stanton, B. A. & Ismailov, II. Gating of
896 amiloride-sensitive Na(+) channels: subunit-subunit interactions and inhibition by the
897 cystic fibrosis transmembrane conductance regulator. *Biophys J* **78**, 1881-1894 (2000).
898 https://doi.org/10.1016/S0006-3495(00)76737-3
899 69 Arganda-Carreras, I. *et al.* Trainable Weka Segmentation: a machine learning tool for
900 microscopy pixel classification. *Bioinformatics* **33**, 2424-2426 (2017).
901 https://doi.org/10.1093/bioinformatics/btx180
902 70 R Core Team (2017) R: A Language and Environment for Statistical Computing.
903 https://www.R-project.org/

904